

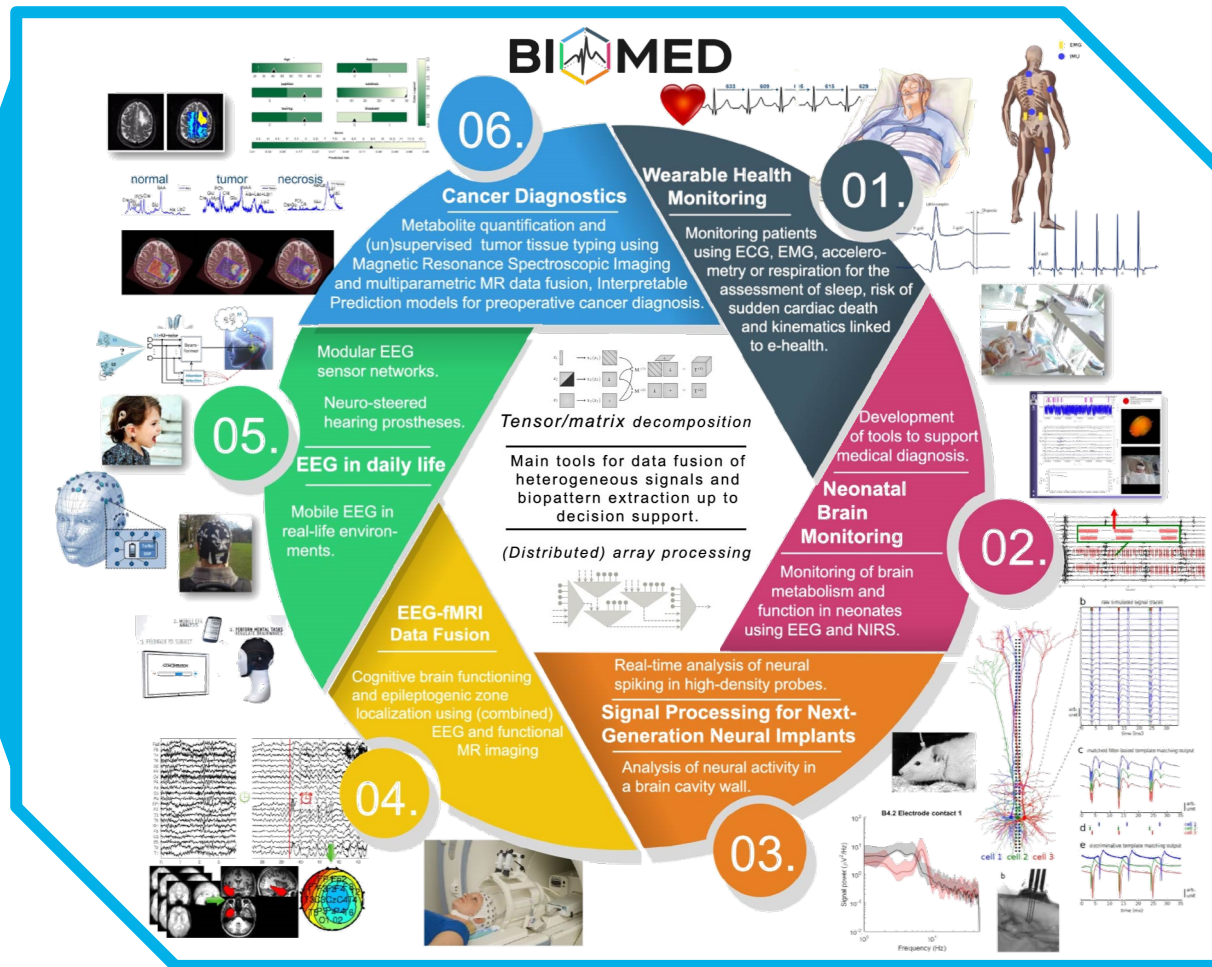


Tensor-based blind source separation of (simultaneous) EEG and fMRI

Borbála Hunyadi



Research in close
collaboration with



| EEG-fMRI data fusion

UZ Leuven Departments:

Radiology

Neurology

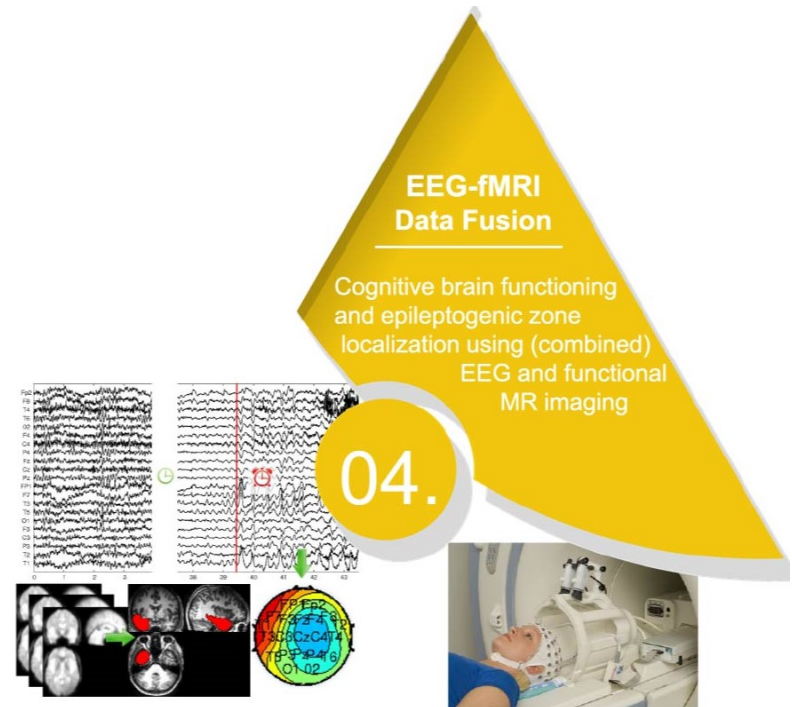
KU Leuven:

Dept. of Psychology

Dept. of Kinesiology and Rehabilitation Sciences

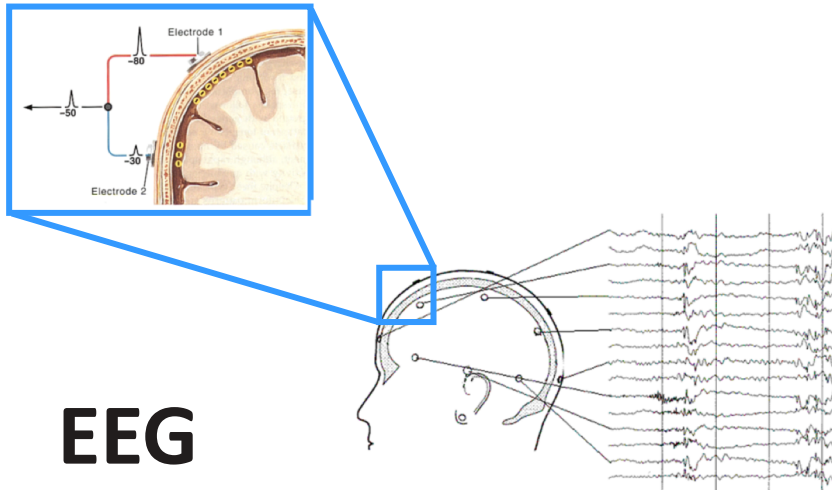
Oxford University:

Dept. of Engineering Science



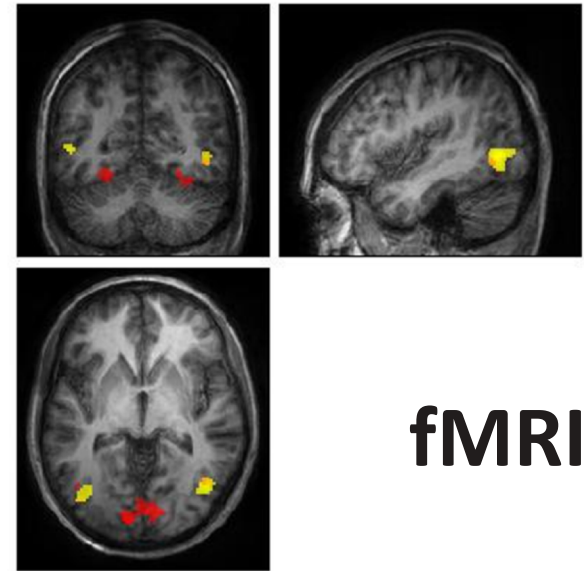
Recording brain activity with EEG and fMRI

EEG measures electrical potentials on the scalp



EEG

fMRI localizes active brain regions



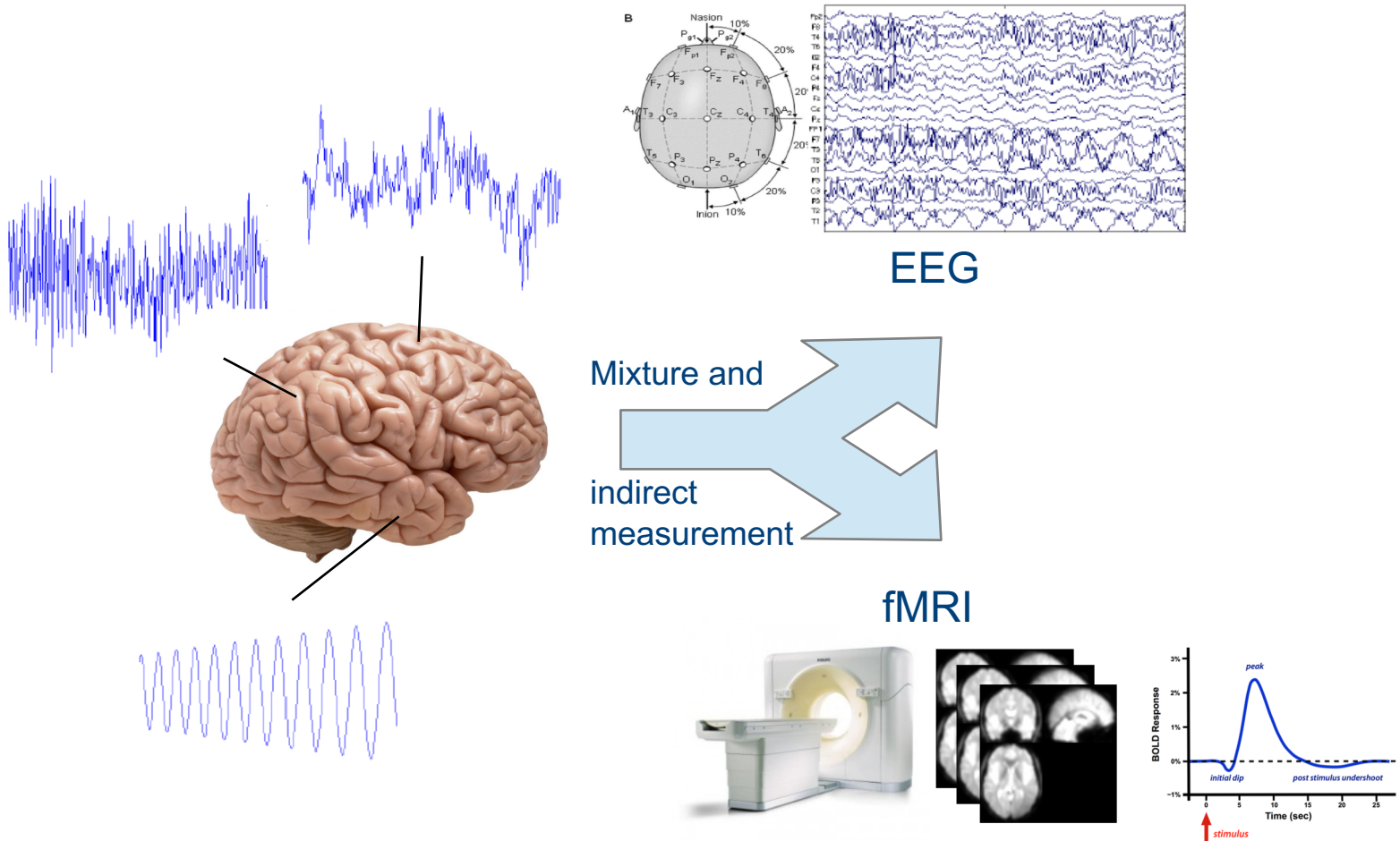
fMRI

Combining EEG and fMRI:

EEG good **temporal resolution** ($\sim ms$)

fMRI good **spatial resolution** ($\sim mm$)

Recording brain activity with EEG and fMRI



Motivation for tensor-based BSS and fusion

- Both EEG and fMRI record a mixture of brain and non-brain signals
- Low SNR → the more information the better
- Complementary in terms of
 - Temporal and spatial resolution
 - Origin of the signal (electrical vs metabolic)

KEYTOOL : Blind source separation

Signal analysis difficult because of artefacts → REMOVE

Matrix based Blind Source Separation (BSS)

- **Non-unique** \rightarrow Constraints are needed (orthogonal, independency)

TENSOR based BSS: unique under mild conditions

ADD extra problem-specific constraints (nonnegative, sparse)

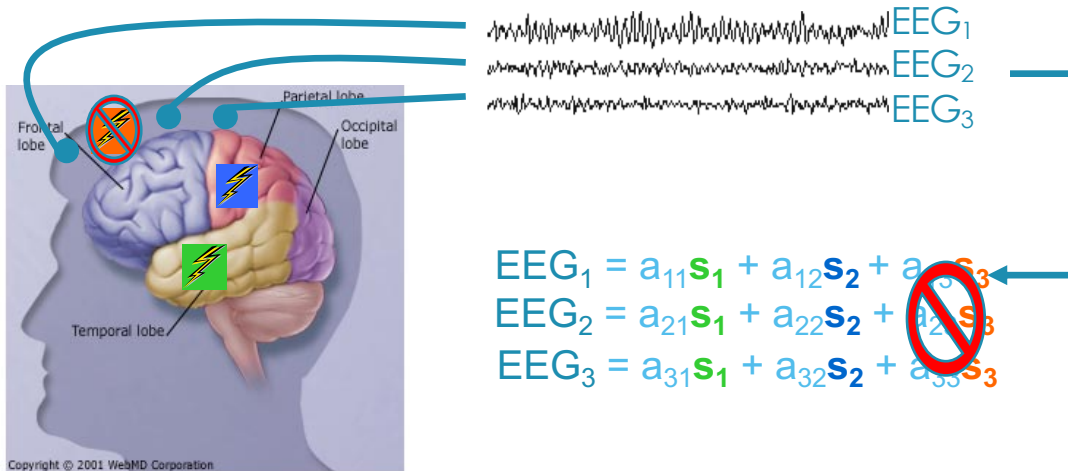


Diagram illustrating the decomposition of a 3D volume \mathcal{X} into a sum of components:

$$\begin{matrix} C \\ P \\ D \end{matrix} \mathcal{X} = \begin{matrix} C_1 \\ \diagdown \end{matrix} B_1 \begin{matrix} \diagup \\ A_1 \end{matrix} + \dots + \begin{matrix} C_R \\ \diagdown \end{matrix} B_R \begin{matrix} \diagup \\ A_R \end{matrix} + \mathcal{E}$$

The diagram shows a 3D box labeled \mathcal{X} with axes C , P , and D . This is equated to a sum of terms. Each term consists of a 3D box with a diagonal line from the top-left corner to the bottom-right corner, labeled C_i on the left and B_i on the right. The bottom-left corner is labeled A_i . The terms are summed from $i=1$ to R , followed by a residual term \mathcal{E} .

Applications

- **Epilepsy**
- Other neurological diseases
 - Sleep disorders
 - Schizophrenia
 - Alzheimer's disease
 - Stroke
- Cognitive science
 - **Task – information processing in the brain**
 - Resting state
- Assistive technologies
 - Consciousness detection
 - **BCI, BMI**
- Commercial
 - Gaming
 - neuroeconomics

Epilepsy surgery

Refractory epilepsy

- ~30% of all epilepsies
- The occurrence of seizures cannot be controlled by medication



Focal epilepsy

- Seizure originates within a certain network in the brain



Surgery

- Key to success: precise **localization** of the epileptogenic zone

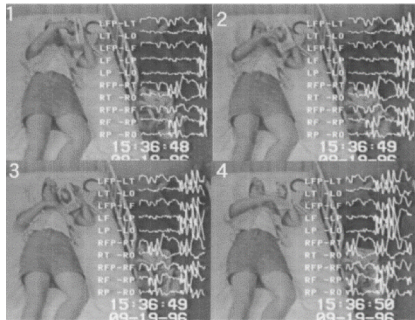


Presurgical evaluation

Epileptogenic zone

- Hypothetical region
- Use of complementary techniques

Ictal Video-EEG monitoring

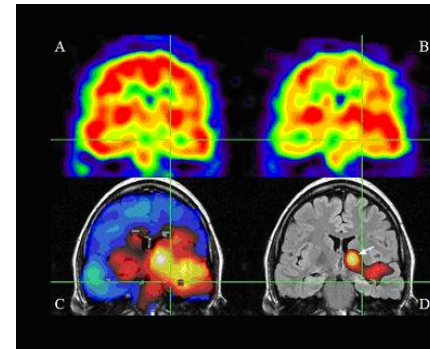


[Y. Shirasaka, T. Mitsuyoshi
Brain and Development 1999]

Interictal EEG-fMRI

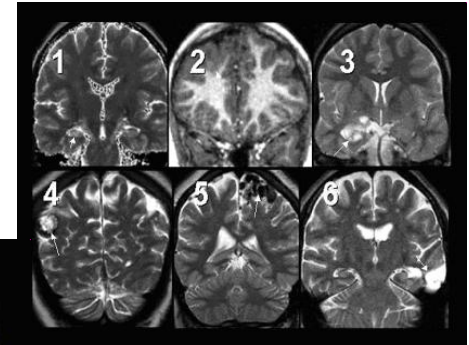


<http://fmri.uib.no/>

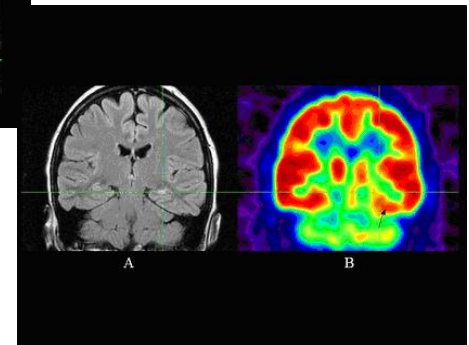


SISCOM

+ Psychological
and psychiatric
evaluation



Structural MRI



PET

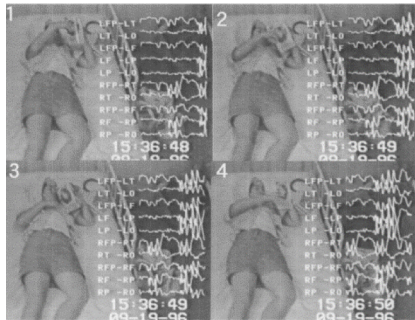
KU LEUVEN

Presurgical evaluation

Epileptogenic zone

- Hypothetical region
- Use of complementary techniques

Ictal Video-EEG monitoring

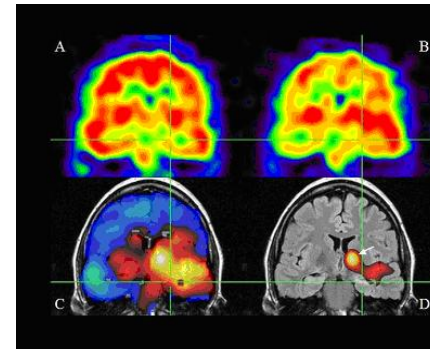


[Y. Shirasaka, T. Mitsuyoshi
Brain and Development 1999]

Interictal EEG-fMRI

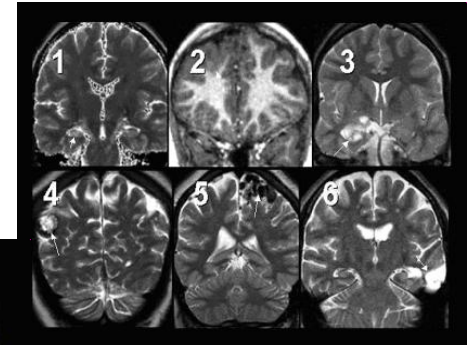


<http://fmri.uib.no/>

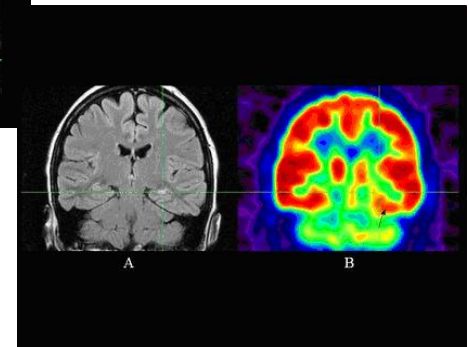


SISCOM

+ Psychological
and psychiatric
evaluation



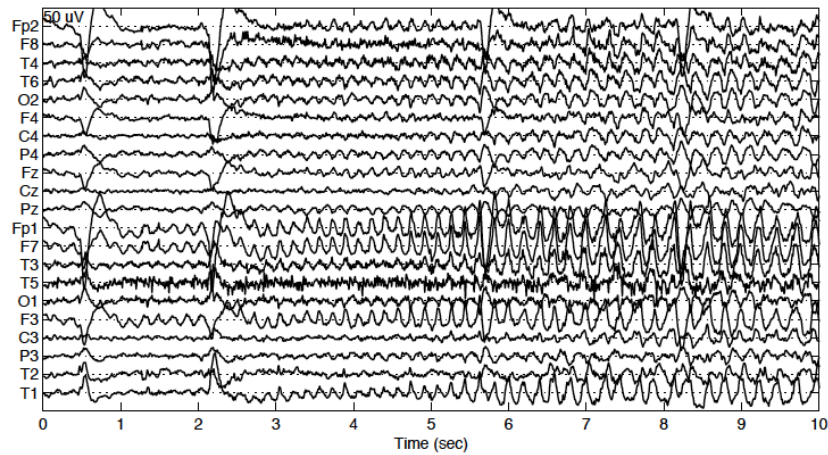
Structural MRI



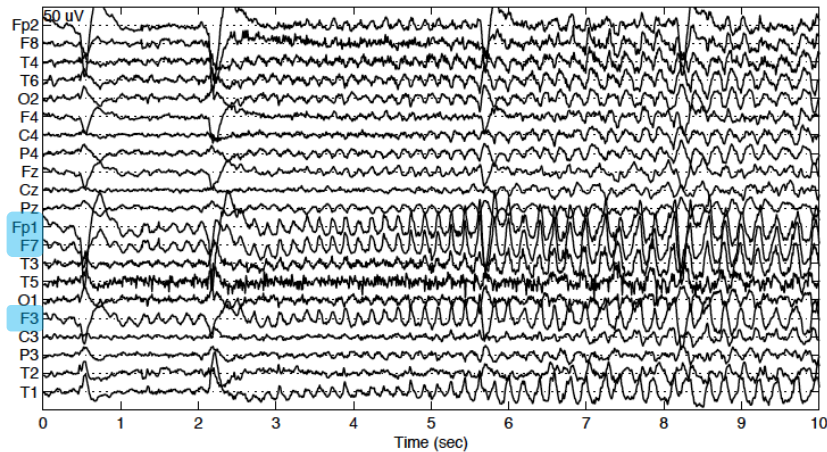
PET

KU LEUVEN

EEG analysis



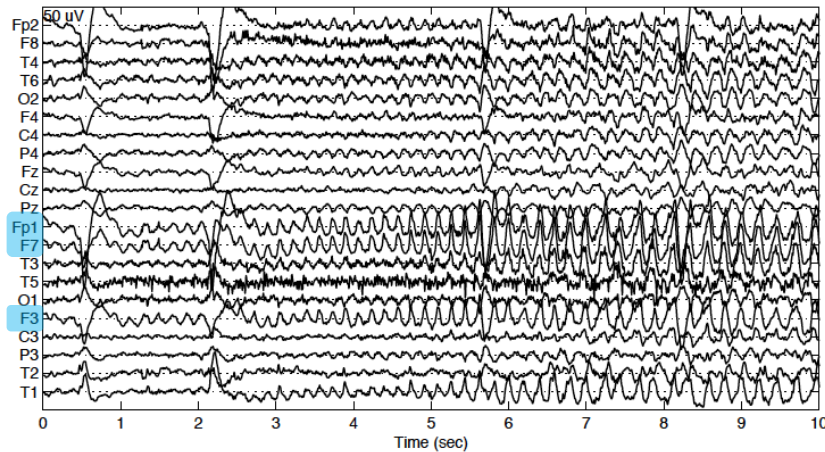
Automated EEG analysis



Goal (clinic):

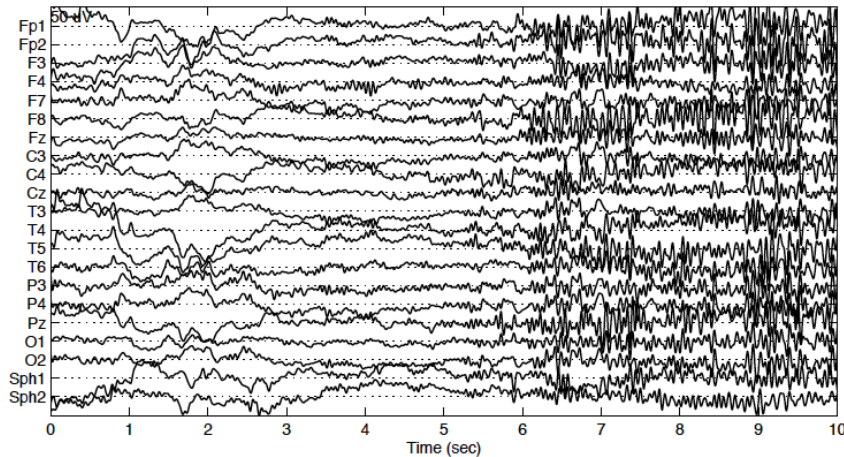
- identify the channels where the seizure originates

Automated EEG analysis



Goal (clinic):

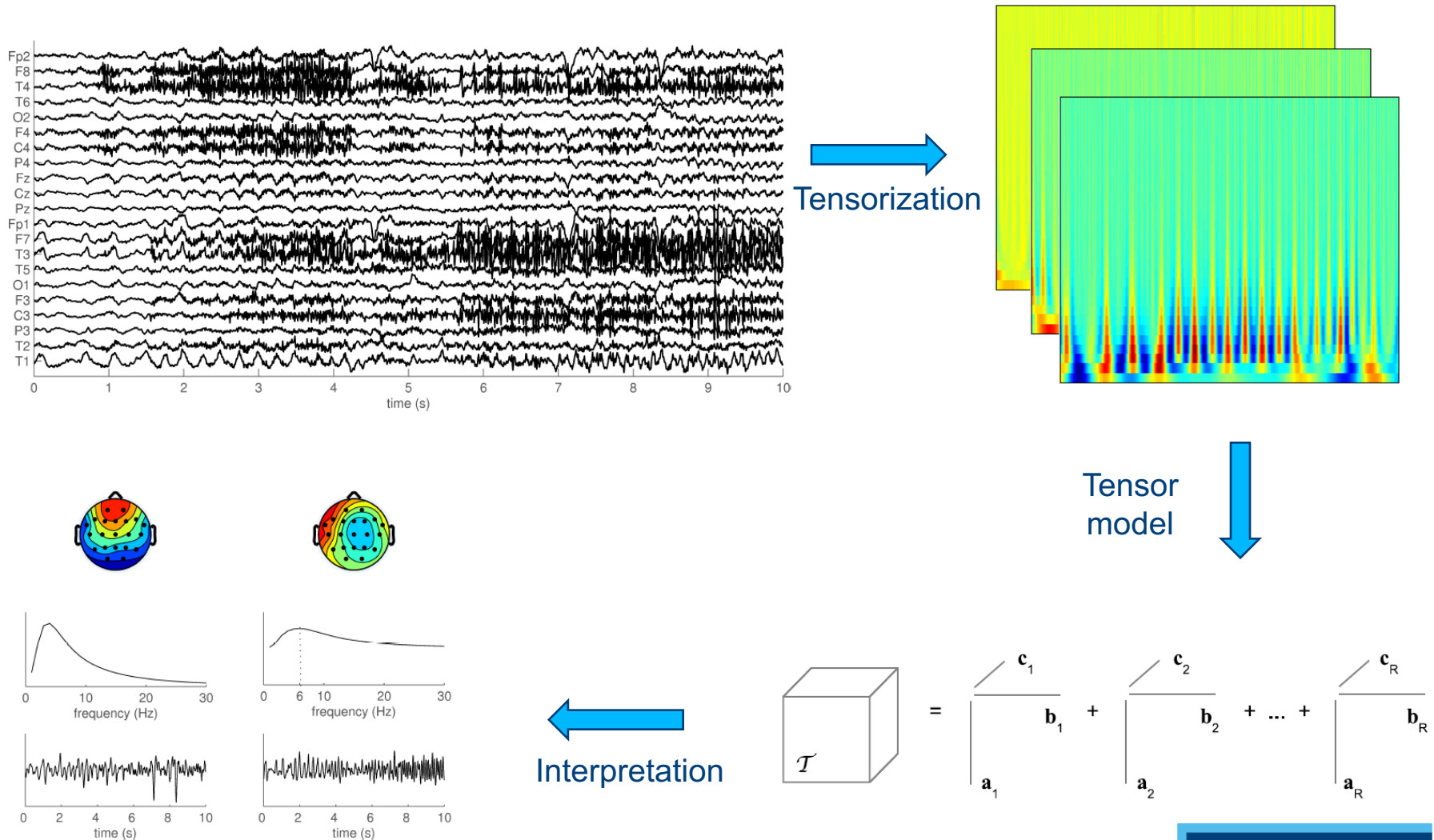
- identify the channels where the seizure originates



Goal (signal processing):

- Automate visual analysis
- Artifact removal

Automated tensor-based EEG analysis



Tensorization and signal model

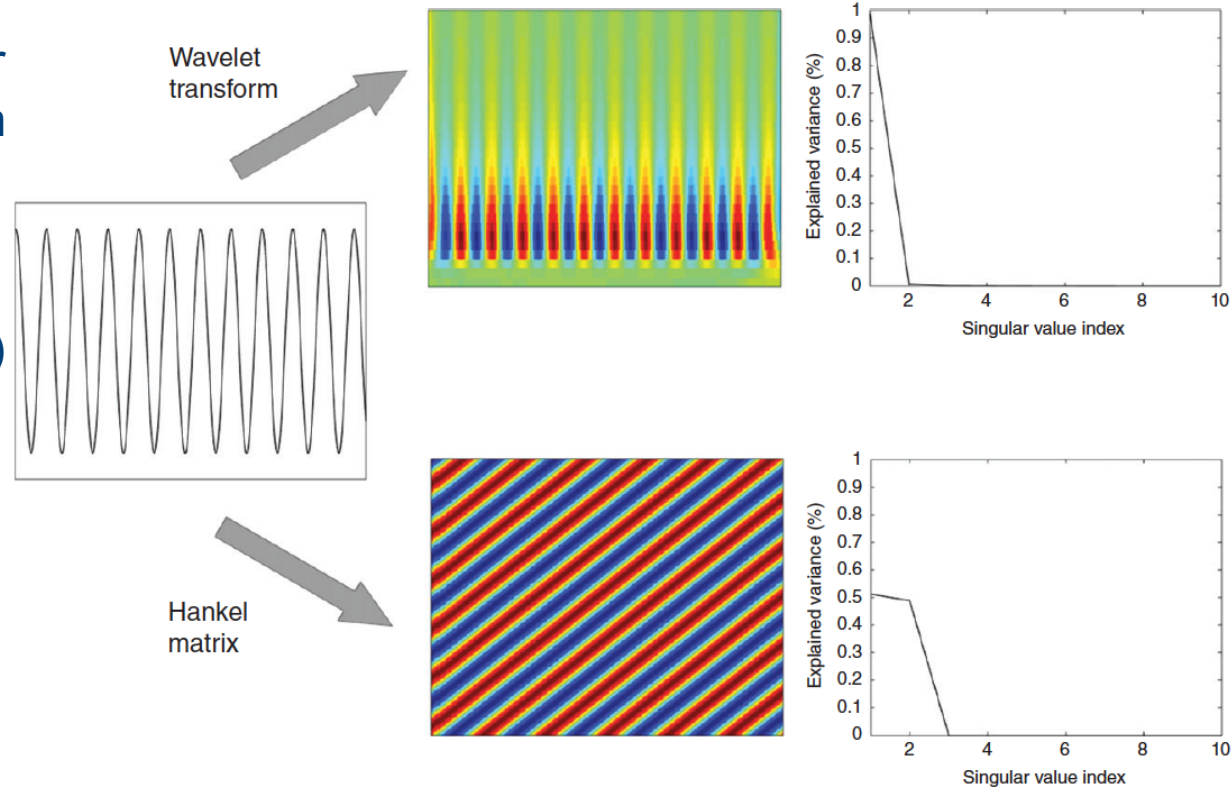
- Time-frequency transformation
(oscillatory patterns)

- Short-time Fourier
- Wavelet transform
- Hilbert-Huang

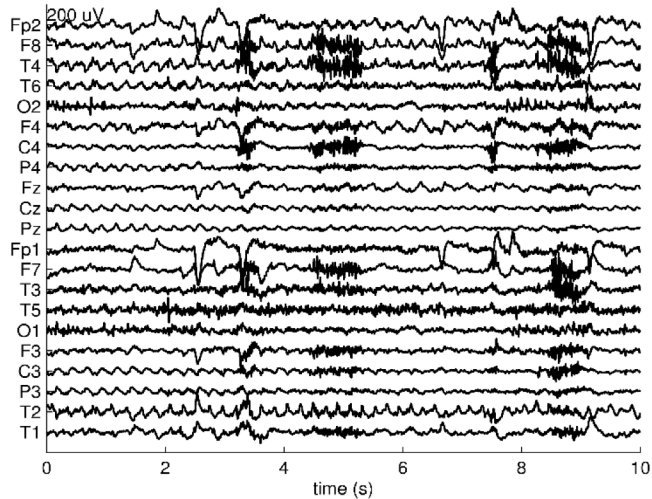
- Hankelization
(sums of exponentials)

- Löwnerization
(rational functions)

- Etc.



Tensor model selection



CPD:

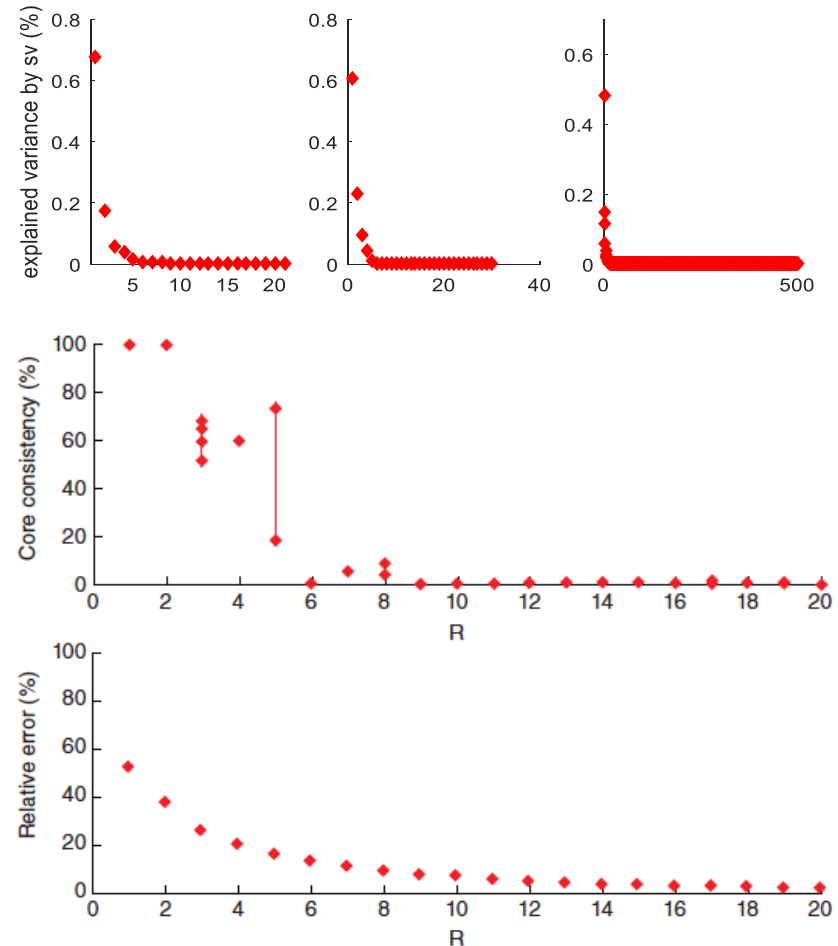
$$\mathcal{T} = \begin{matrix} \text{c}_1 \\ \text{b}_1 \\ \text{a}_1 \end{matrix} + \begin{matrix} \text{c}_2 \\ \text{b}_2 \\ \text{a}_2 \end{matrix} + \dots + \begin{matrix} \text{c}_R \\ \text{b}_R \\ \text{a}_R \end{matrix}$$

[Acar et al. 2007,
De Vos et al 2007]

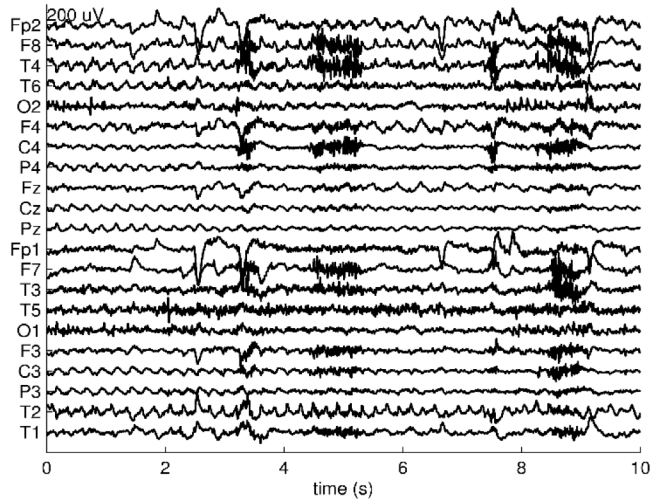
?

Tensor model selection

- Inspect multilinear singular values
- Vary R and inspect
 - Explained variance
 - Core consistency
- Run the model multiple times
 - Different initializations
 - Verify uniqueness



Tensor model selection



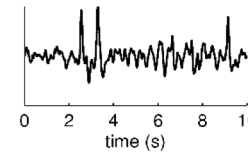
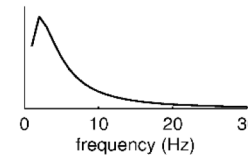
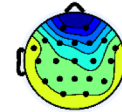
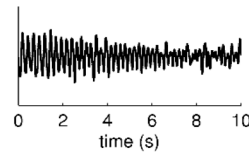
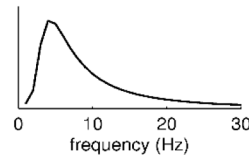
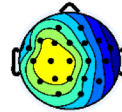
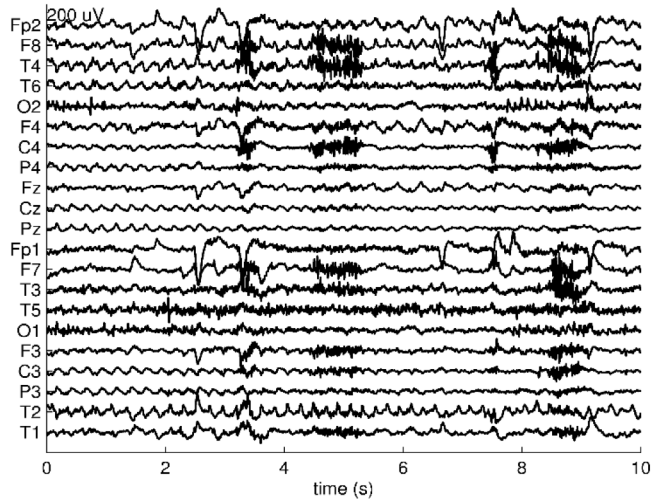
CPD:

$$\mathcal{T} = \begin{matrix} c_1 \\ \hline b_1 \\ \hline a_1 \end{matrix} + \begin{matrix} c_2 \\ \hline b_2 \\ \hline a_2 \end{matrix} + \dots + \begin{matrix} c_R \\ \hline b_R \\ \hline a_R \end{matrix}$$

[Acar et al. 2007,
De Vos et al 2007]

?

Tensor model selection



Diagnostic information:

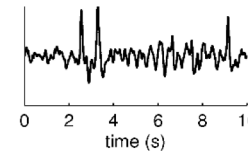
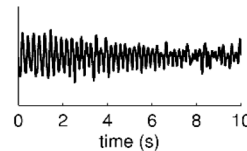
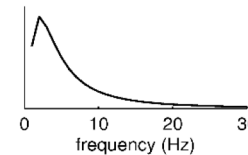
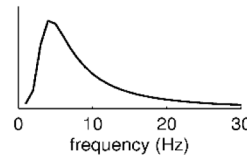
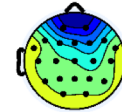
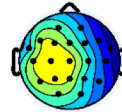
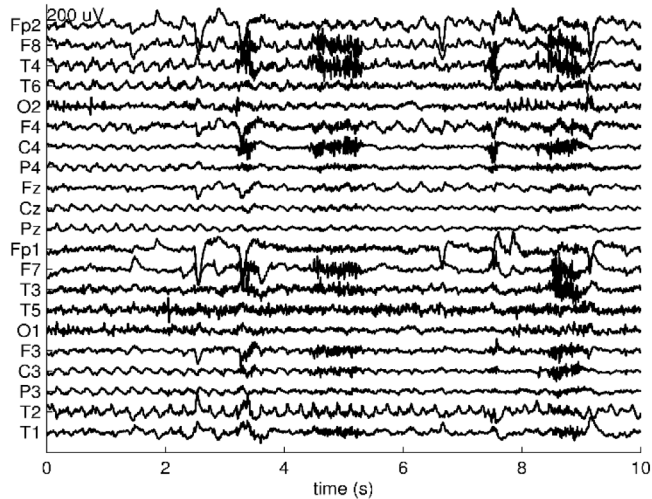
- morphology
- topography
- frequency

CPD:

$$\mathcal{T} = \begin{matrix} & c_1 \\ \begin{matrix} a_1 \\ b_1 \end{matrix} & \end{matrix} + \begin{matrix} & c_2 \\ \begin{matrix} a_2 \\ b_2 \end{matrix} & \end{matrix}$$

[Acar et al. 2007,
De Vos et al 2007]

Tensor model selection



Diagnostic information:

- morphology
- topography
- frequency

CPD:

$$\mathcal{T} = \begin{matrix} & c_1 \\ \begin{matrix} a_1 \\ b_1 \end{matrix} & \end{matrix} + \begin{matrix} & c_2 \\ \begin{matrix} a_2 \\ b_2 \end{matrix} & \end{matrix}$$

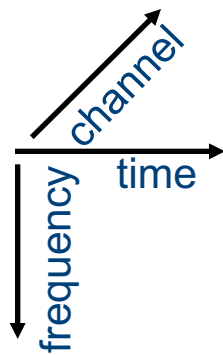
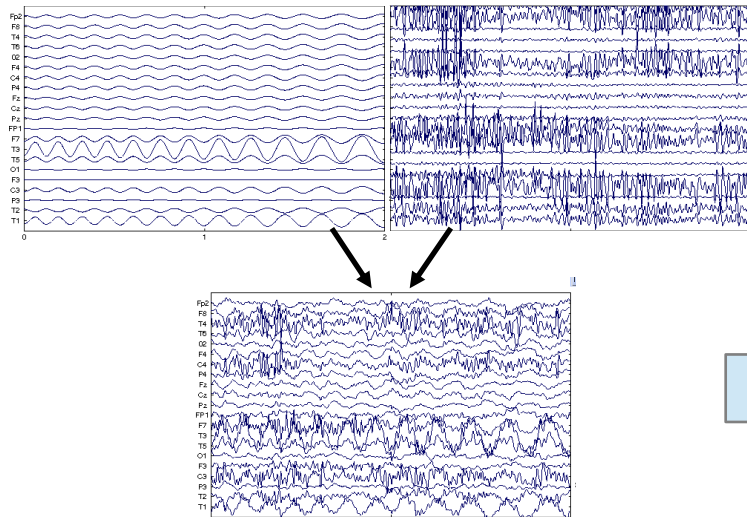
[Acar et al. 2007,
De Vos et al 2007]

BTD-(L,L,1):

$$\mathcal{T} = \begin{matrix} I_3 \\ I_2 \\ I_1 \end{matrix} = \begin{matrix} I_3 \\ I_2 \\ I_1 \end{matrix} \begin{matrix} c_1 \\ B_1^T \\ A_1 \end{matrix} L_1 + \begin{matrix} I_3 \\ I_2 \\ I_1 \end{matrix} \begin{matrix} c_2 \\ B_2^T \\ A_2 \end{matrix} L_2 + \dots + \begin{matrix} I_3 \\ I_2 \\ I_1 \end{matrix} \begin{matrix} c_R \\ B_R^T \\ A_R \end{matrix} L_R$$

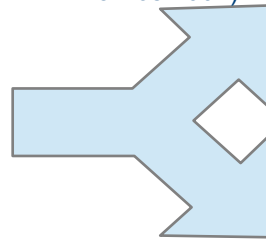
[Hunyadi et al 2014]

Signal model: oscillatory pattern



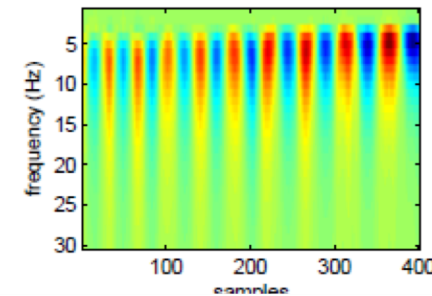
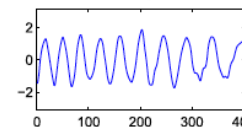
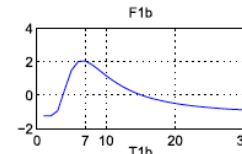
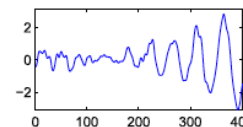
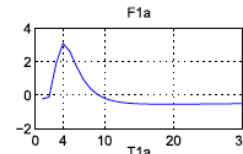
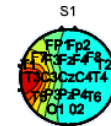
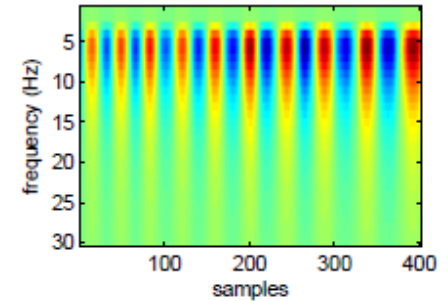
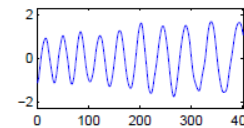
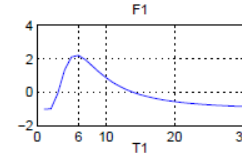
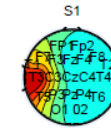
CWT-CPD

(Acar 2007,
De Vos 2007)

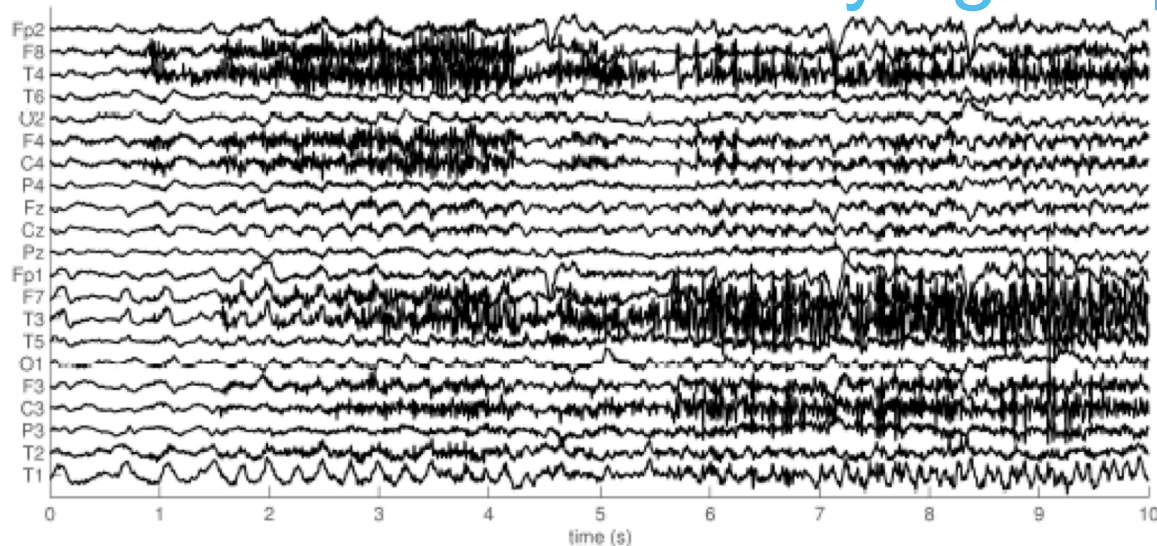


CWT-BTD

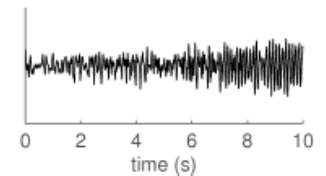
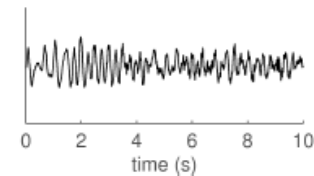
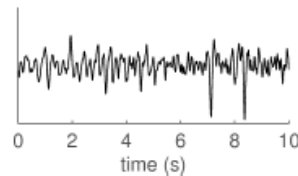
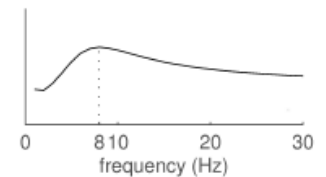
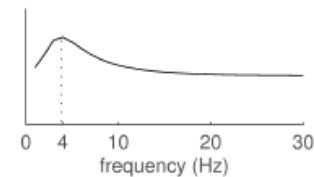
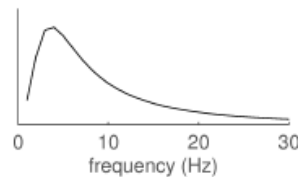
(Hunyadi et al 2014)



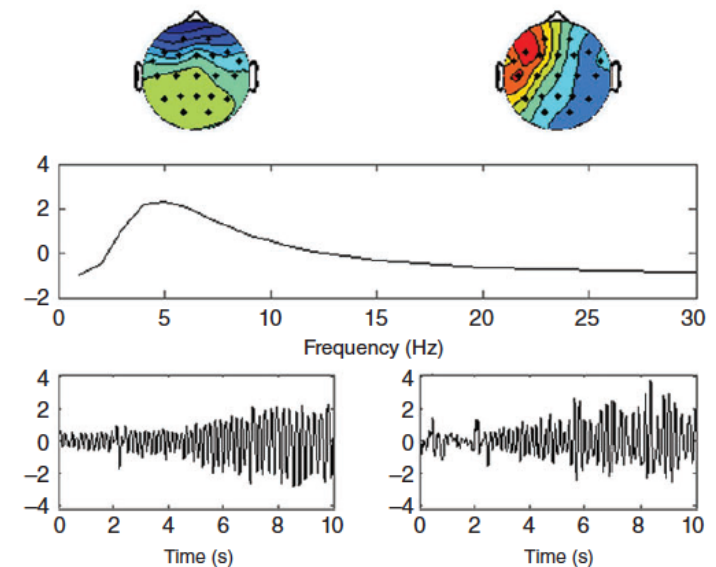
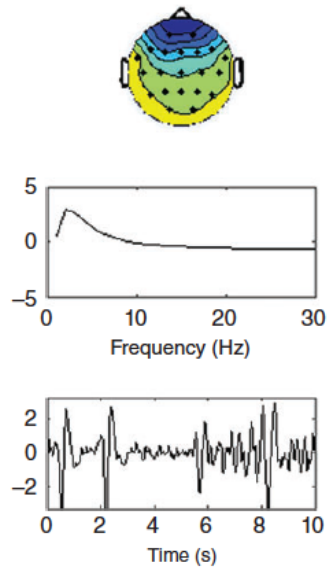
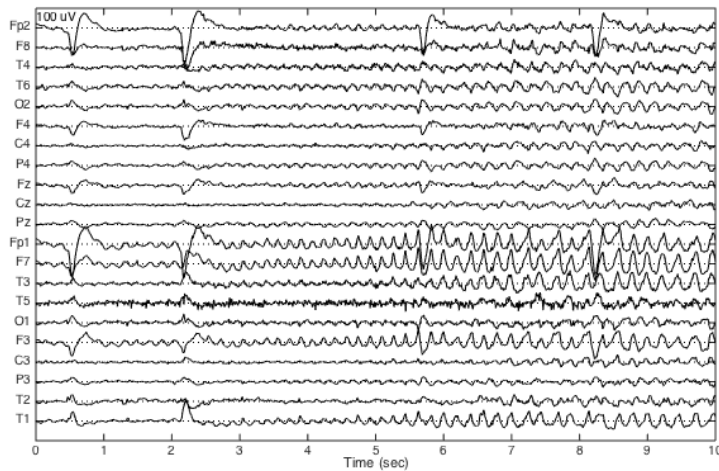
BTD of seizure 1: varying frequency



(a) Raw EEG

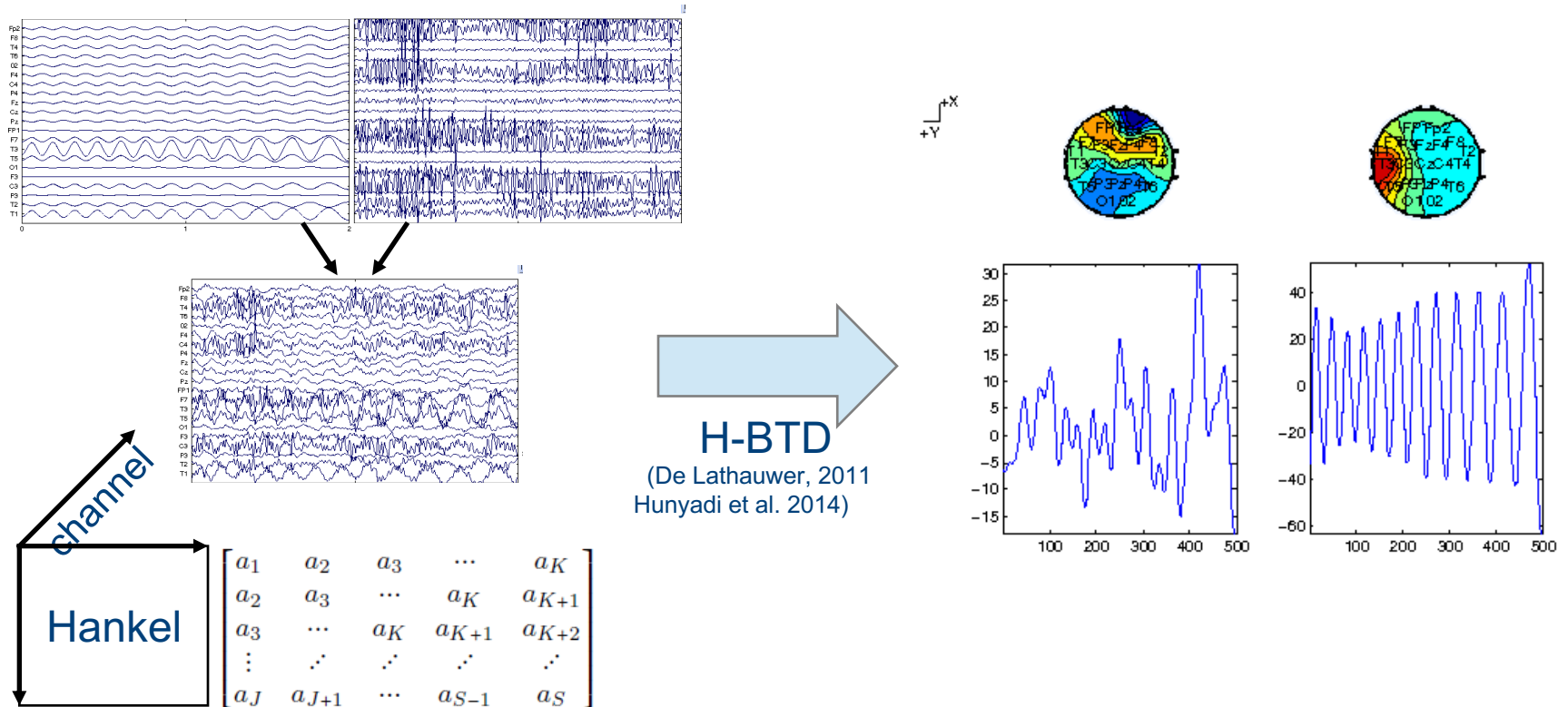


BTD of seizure 2: varying source



Signal model: sum of exp. damped sinusoids

BTD of Hankel expanded tensors



Signal model: sum of exp. damped sinusoids

$$s_r(n) = \sum_{l_r=1}^{L_r} c_{l_r,r} z_{l_r,r}^n, \text{ with } 0 \leq n \leq N-1, 1 \leq r \leq R.$$

Sources: sum of exponentials

$$e^{-\alpha n} \cos(\omega n + \phi) = cz^n + c^*(z^*)^n, \text{ with } c = \frac{1}{2}e^{j\phi}$$

$$z = e^{-\alpha + j\omega}$$

Special case: sum of damped sinusoids

$$\mathbf{a}_{ch} = [a_{ch}(1) \ a_{ch}(2) \ \dots \ a_{ch}(S)],$$

Hankelization

$$\mathbf{H}_{ch} = \begin{bmatrix} a_{ch}(1) & a_{ch}(2) & a_{ch}(3) & \dots & a_{ch}(K) \\ a_{ch}(2) & a_{ch}(3) & \dots & a_{ch}(K) & a_{ch}(K+1) \\ a_{ch}(3) & \dots & a_{ch}(K) & a_{ch}(K+1) & a_{ch}(K+2) \\ \vdots & \ddots & \ddots & \ddots & \ddots \\ a_{ch}(J) & a_{ch}(J+1) & \dots & a_{ch}(S-1) & a_{ch}(S) \end{bmatrix}$$

$$\text{Rank}(\mathbf{H}) = L_r$$

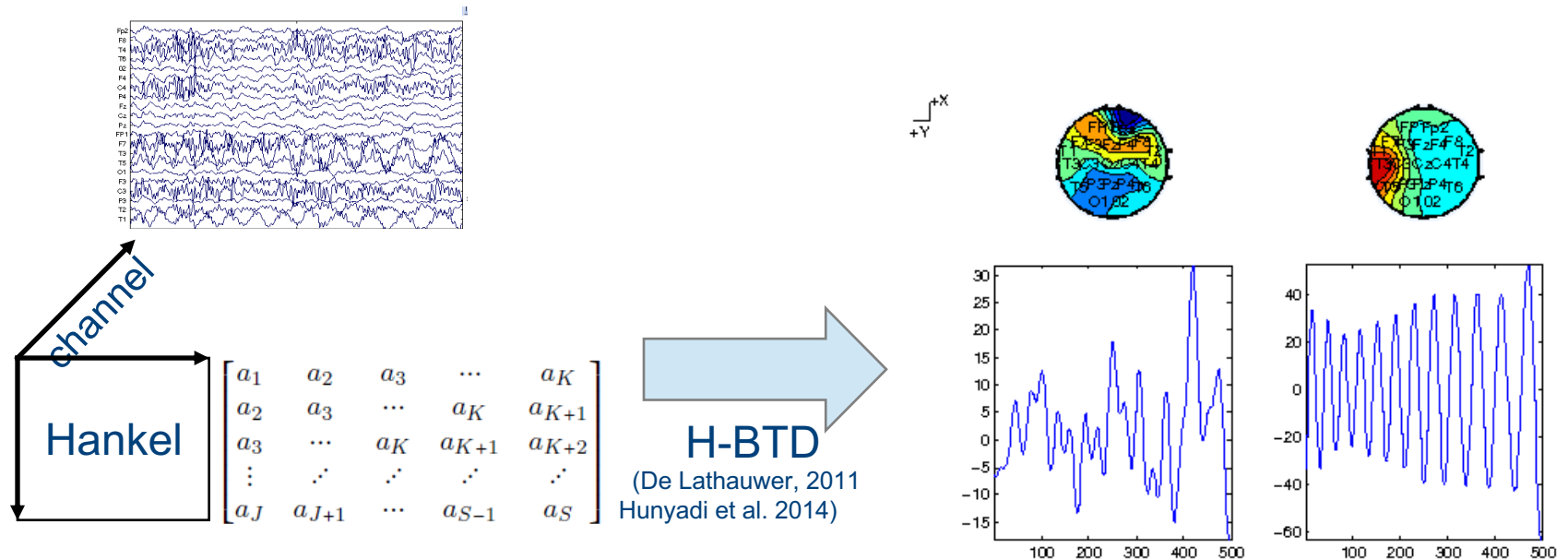
Linear
combination
of sources

$$\mathbf{H}_r = \mathbf{V}_r \cdot \text{diag}(c_{1,r}, c_{2,r}, \dots, c_{L_r,r}) \cdot \hat{\mathbf{V}}_r^T,$$

$$\mathbf{V}_r = \begin{bmatrix} 1 & 1 & \dots & 1 \\ z_{1,r} & z_{2,r} & \dots & z_{L_r,r} \\ \vdots & \vdots & \ddots & \vdots \\ z_{1,r}^{J-1} & z_{2,r}^{J-1} & \dots & z_{L_r,r}^{J-1} \end{bmatrix}, \hat{\mathbf{V}}_r = \begin{bmatrix} 1 & 1 & \dots & 1 \\ z_{1,r} & z_{2,r} & \dots & z_{L_r,r} \\ \vdots & \vdots & \ddots & \vdots \\ z_{1,r}^{J-1} & z_{2,r}^{J-1} & \dots & z_{L_r,r}^{J-1} \end{bmatrix}$$

Signal model: sum of exp. damped sinusoids

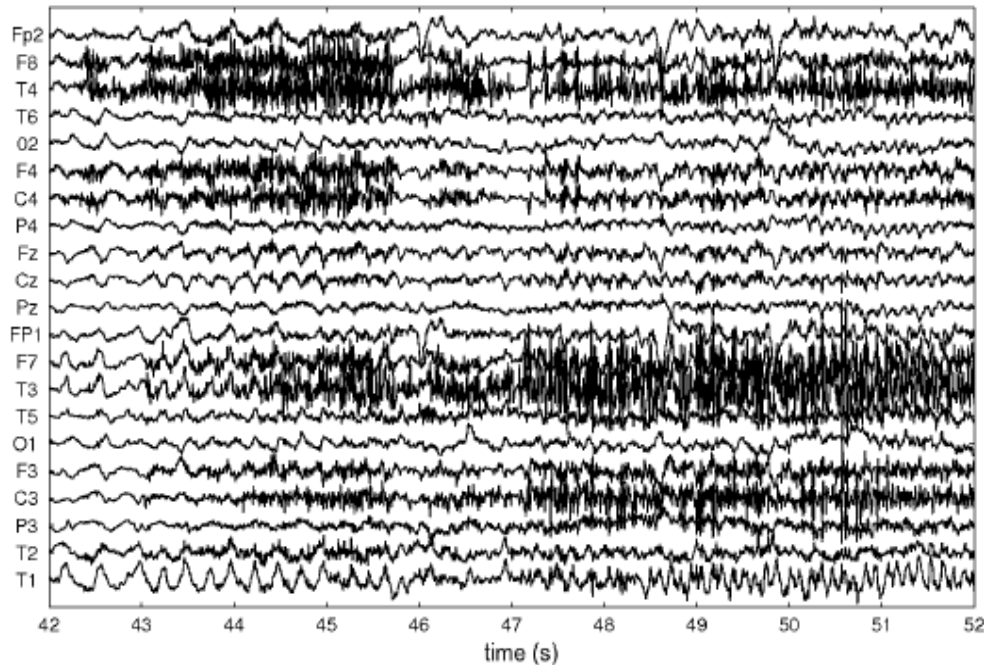
BTD of Hankel expanded tensors



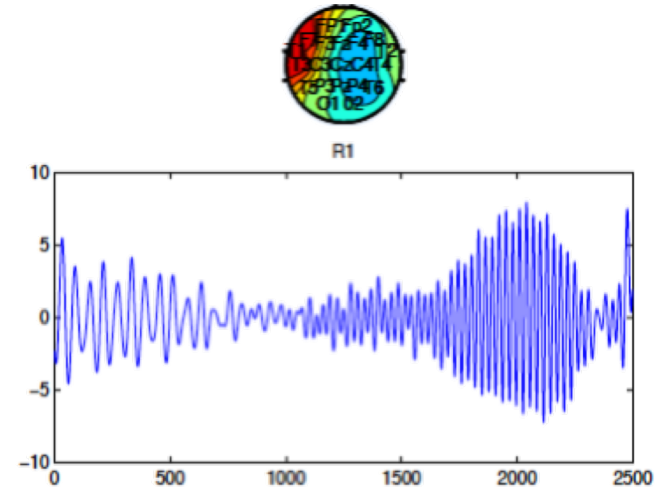
BTD-(L,L,1):

$$\begin{array}{c} I_3 \\ I_2 \\ I_1 \\ \mathcal{T} \end{array} = \begin{array}{c} I_3 \\ I_1 \\ \mathbf{A}_1 \end{array} \begin{array}{c} \mathbf{B}_1^T \\ I_2 \\ L_1 \end{array} + \begin{array}{c} I_3 \\ I_1 \\ \mathbf{A}_2 \end{array} \begin{array}{c} \mathbf{B}_2^T \\ I_2 \\ L_2 \end{array} + \dots + \begin{array}{c} I_3 \\ I_1 \\ \mathbf{A}_R \end{array} \begin{array}{c} \mathbf{B}_R^T \\ I_2 \\ L_R \end{array}$$

H-BTD of seizure 1



(a) Raw EEG

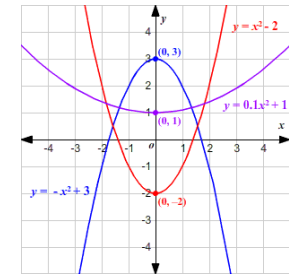
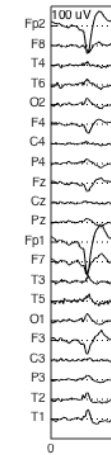


(d) H-BTD

$L_r=6$

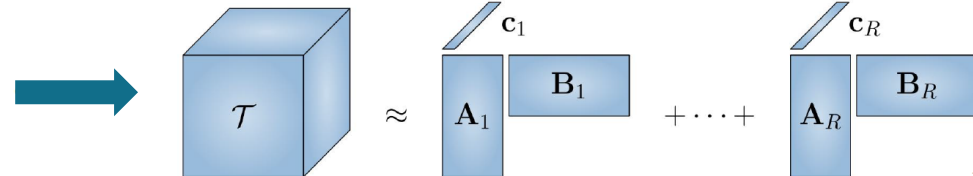
Eye blink artifact

- If too L too high, the seizure and eye blink component will be intermixed
- See demo!
- Solution:
 - Model and remove eye blink before performing H-BTD
 - Eye blink ~ quadratic function
 - Löwnerization: $f(x)$ sampled at two distinct points sets $X=\{x_1, x_2, \dots, x_I\}$ and $Y=\{y_1, y_2, \dots, y_J\}$



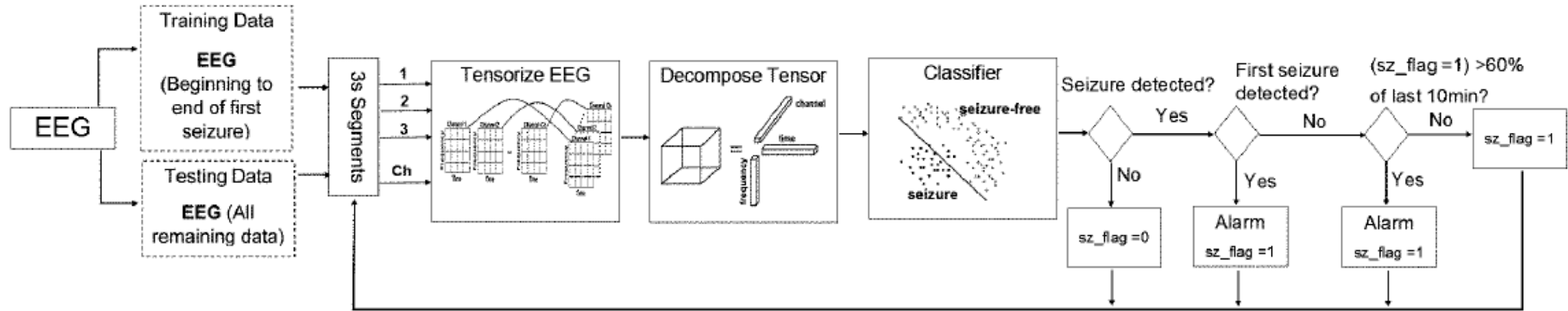
$$\mathbf{L} = \begin{bmatrix} \frac{f(x_1)-f(y_1)}{x_1-y_1} & \frac{f(x_1)-f(y_2)}{x_1-y_2} & \dots & \frac{f(x_1)-f(y_J)}{x_1-y_J} \\ \frac{f(x_2)-f(y_1)}{x_2-y_1} & \frac{f(x_2)-f(y_2)}{x_2-y_2} & \dots & \frac{f(x_2)-f(y_J)}{x_2-y_J} \\ \vdots & \vdots & \ddots & \vdots \\ \frac{f(x_I)-f(y_1)}{x_I-y_1} & \frac{f(x_I)-f(y_2)}{x_I-y_2} & \dots & \frac{f(x_I)-f(y_J)}{x_I-y_J} \end{bmatrix}$$

$$\text{rank}(\mathbf{L}) = \delta = \deg(f).$$

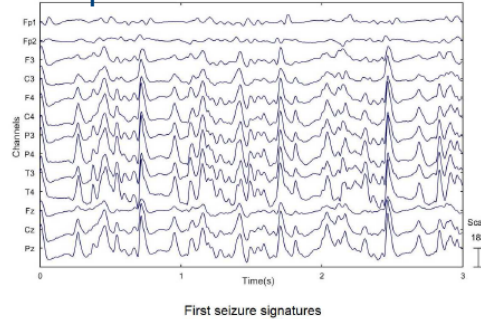


19

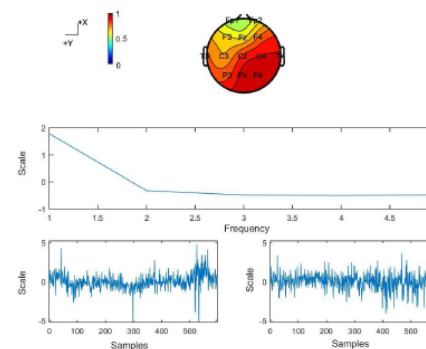
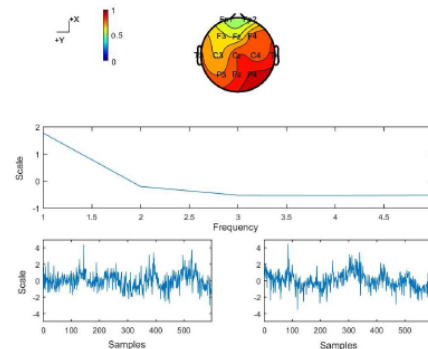
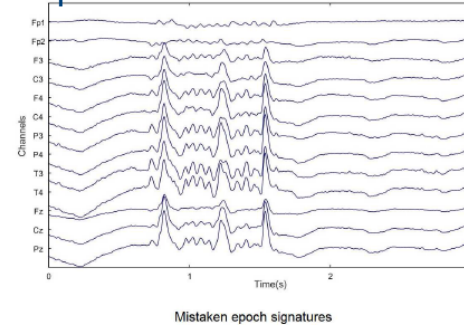
Application: automated seizure detection



Epoch from first seizure



Epoch classified as seizure



[Rodriguez Aldana 2017]

Application: Localization of seizure onset zone

1. Few seizures -> long hospital stay
2. EEG resolution not great
3. Epileptic activity in deep structures not picked up

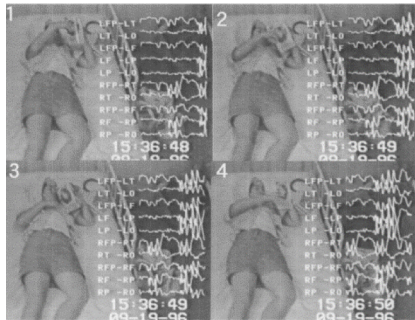
Therefore...

Presurgical evaluation

Epileptogenic zone

- Hypothetical region
- Use of complementary techniques

Ictal Video-EEG monitoring

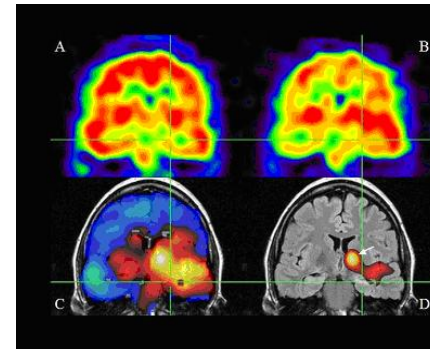


[Y. Shirasaka, I. Mitsuyoshi
Brain and Development 1999]

Interictal EEG-fMRI

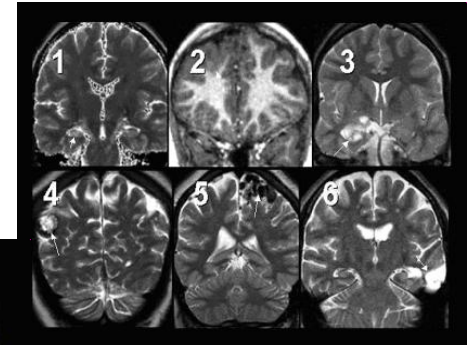


<http://fmri.uib.no/>

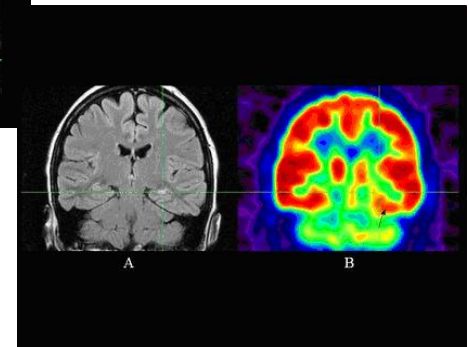


SISCOM

+ Psychological
and psychiatric
evaluation



Structural MRI



PET

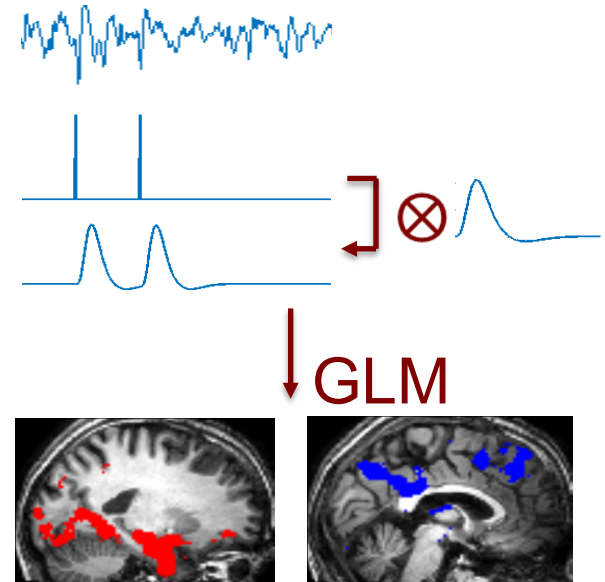
KU LEUVEN

EEG-correlated fMRI

1. Find interictal spikes on EEG
2. Create a vector of spike timing
3. Create a regressor by convolving the timing vector with the HRF
4. Create regressors based on various confounders (e.g. head movement)
5. Analyze fMRI time series within the general linear model (GLM):

$$Y = X\beta + e$$

6. Solution in the LS sense:
$$\beta = (X^T X)^{-1} X^T y + e$$
7. Activation maps are obtained by statistical hypothesis testing of β values



EEG-correlated fMRI

Success stories:

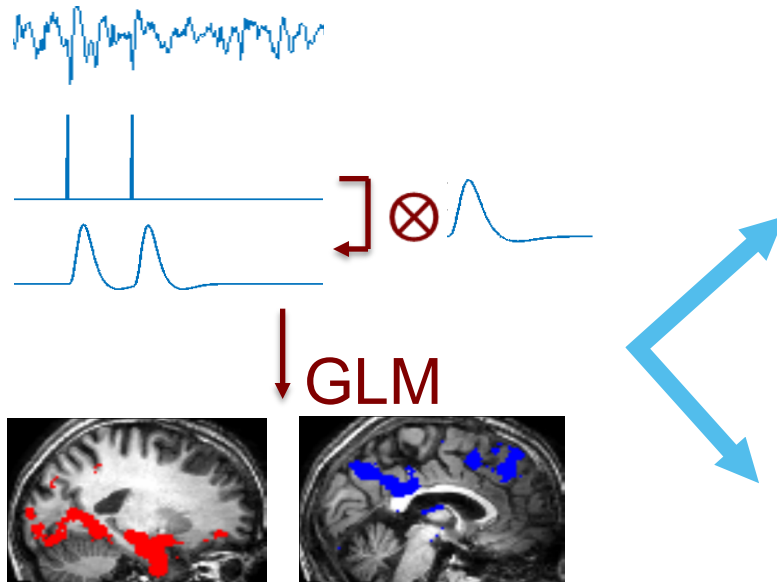
- IED-related BOLD changes in focal and generalized epilepsy [*Gotman 2006*]
- Instrumental in presurgical evaluation [*Zijlmans 2007, Pittau 2012*]

Hypothetically, the network is:

- active during interictal spikes
- focal and coincides with the true epileptogenic zone

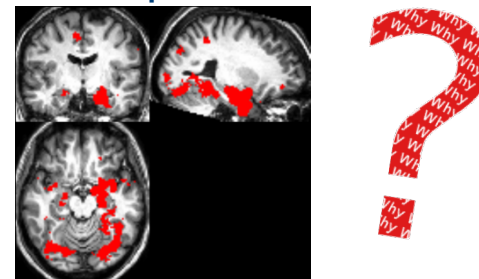
But...

EEG-correlated fMRI



40-70% EEG-fMRI studies fail
due to lack of interictal spikes
[Grouiller et al. 2011]

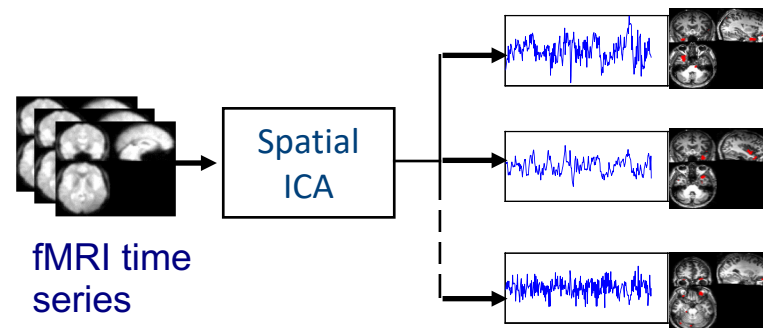
Widespread activation



ICA of interictal fMRI

[Rodionov et al 2007]

- EEG-positive cases
- Selection based on temporal regressor and GLM-based activation map



Spatial ICA vs Temporal ICA

- Temporal ICA: used in EEG
- fMRI: too few time points for robust statistics in the temporal mode
- fMRI Spatial mode:
 - vectorization of the 3D volume of voxels
 - Voxel x time matrices
 - Independence in the voxel mode: super-Gaussian distributions (Infomax); high kurtosis (fastICA)

$$X_{\text{fMRI}} = A_{\text{fMRI}} S_{\text{fMRI}}$$

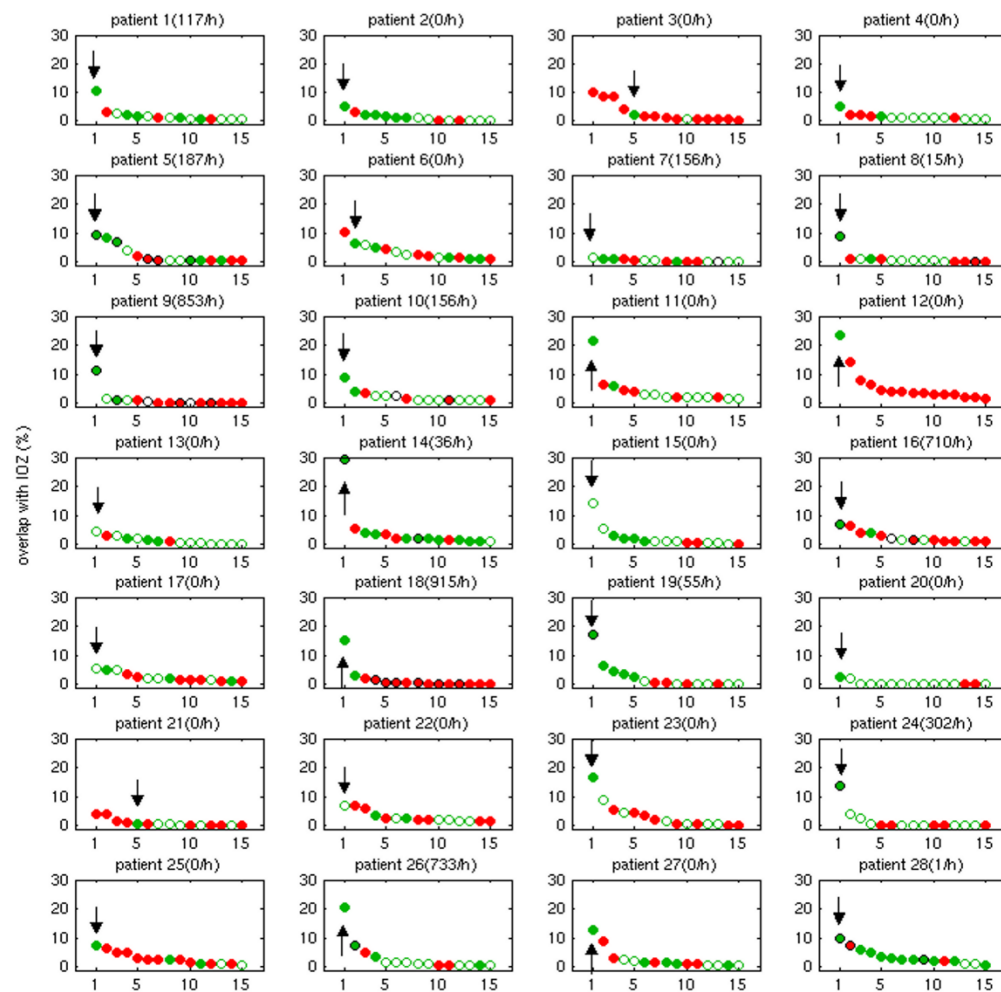
ICA of EEG-negative fMRI

- Data acquisition:
 - Simultaneous EEG-fMRI recordings
 - 10-22 minute long sessions
 - 2-4 sessions per individual
 - 28 patients refractory epilepsy patients
 - Presurgical evaluation → concordant results → known EZ
 - EEG-positive group: 11 had clinically concordant spikes
 - EEG-negative group: 17 patient had no clinically concordant spikes
 - 12 healthy controls
- Analysis:
 - Group ICA on all sessions for each individual separately
 - Overlap between each IC and known EZ
 - Artifact-related ICs rejected manually

ICA of EEG-negative fMRI

Results:

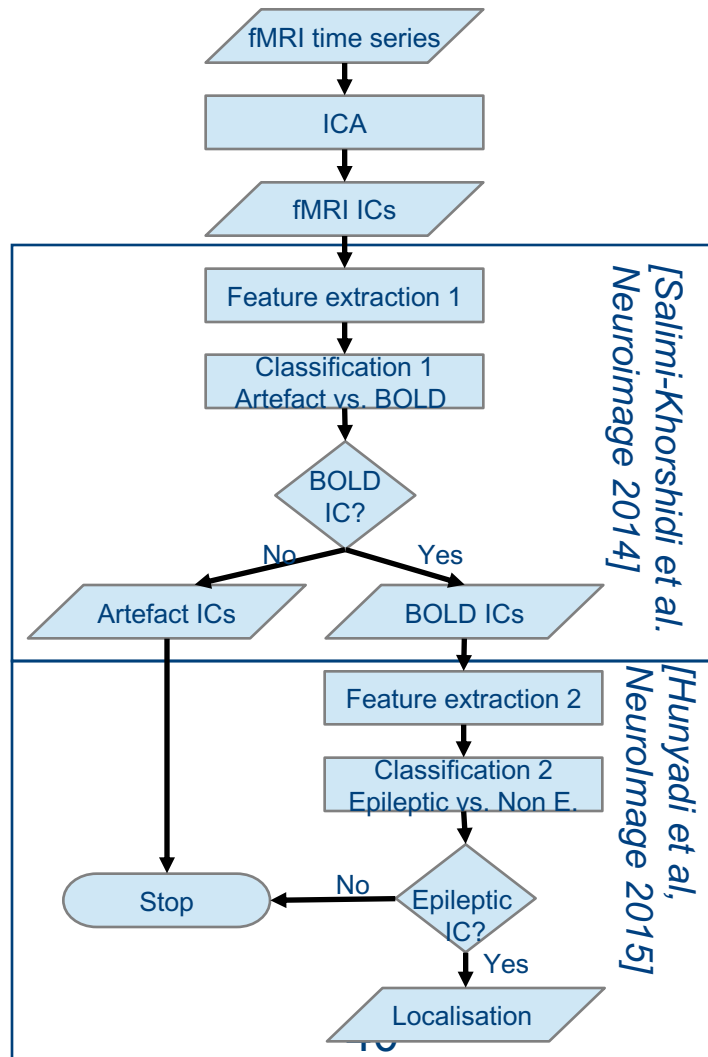
- Epileptic IC (\downarrow , eIC) was identified as the IC with the largest overlap with the EZ, after excluding artefacts (\bullet).
- ICA revealed epileptic sources overlapping with the EZ also in patients without spikes.
- Overlaps are significantly larger than in control group



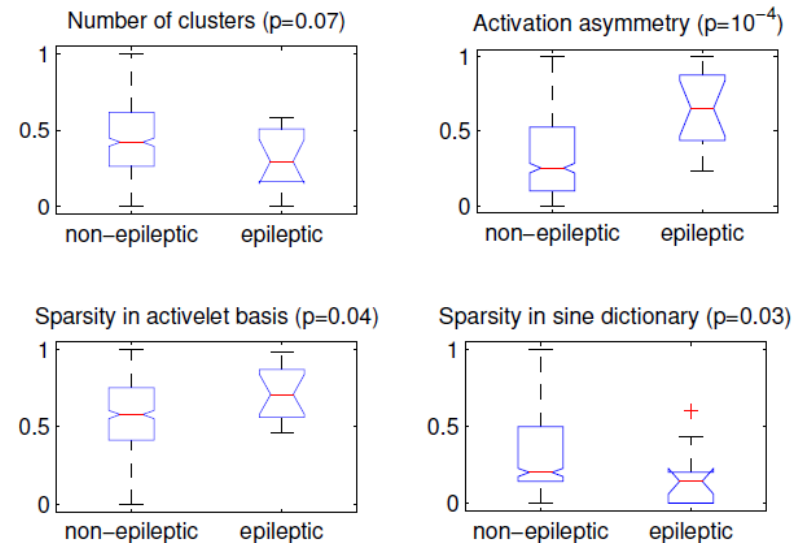
[Hunyadi et al 2013]

component index

Selecting the epileptic IC



Feature extraction 2:



Classification 2:

- LS-SVM with linear kernel and modified decision function:

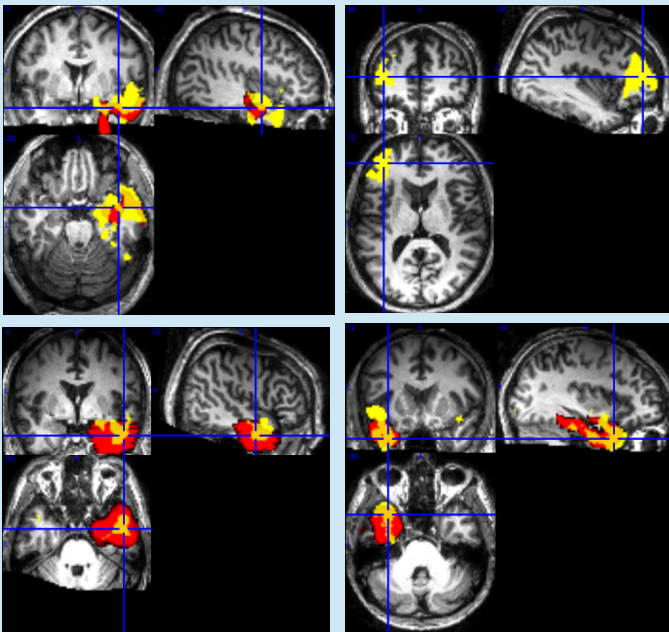
$$y(x_i) = \begin{cases} 1 & \text{if } \arg \max_{\mathbf{x}} (\mathbf{w}^T \boldsymbol{\varphi}(\mathbf{x})) = i \text{ and } \mathbf{w}^T \boldsymbol{\varphi}(\mathbf{x}) + b > 0 \\ 0 & \text{otherwise.} \end{cases}$$

Outcome in EEG-negative cases

- Training set: 12 EEG-positive cases
- A selection was made in 1 out of 13 controls: 92% specificity
- A selection was made in 11 out of 18 patients

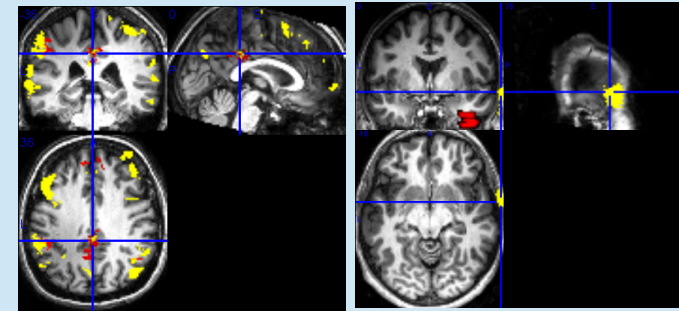
Informative (4)

Concordant with the EZ (4)



Misleading (0)

Non-informative (7)



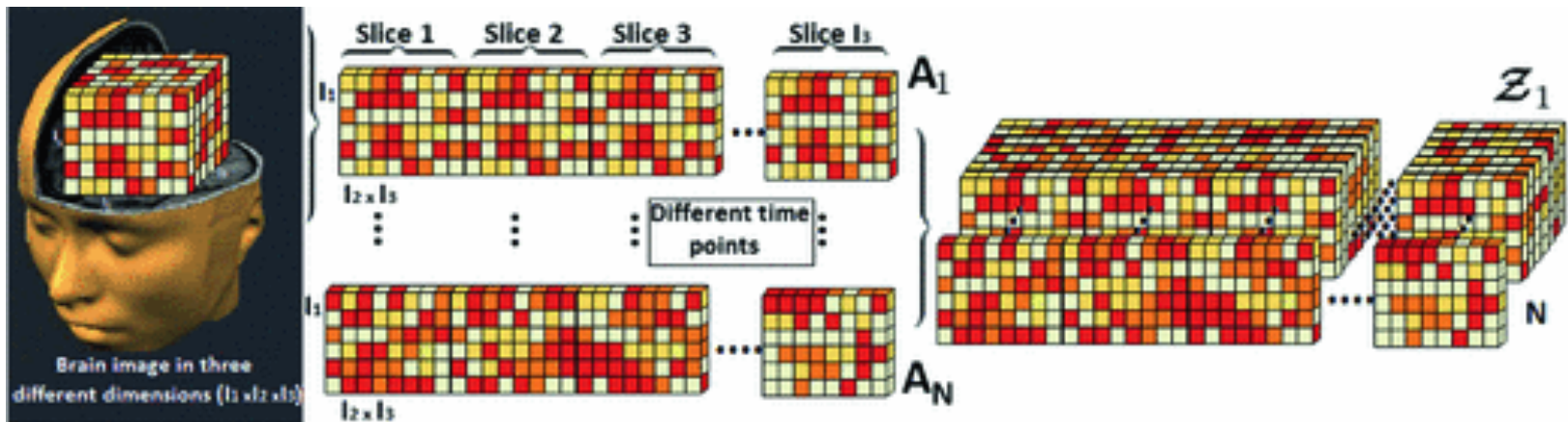
ECN (average of 6 selected maps)

Artefact

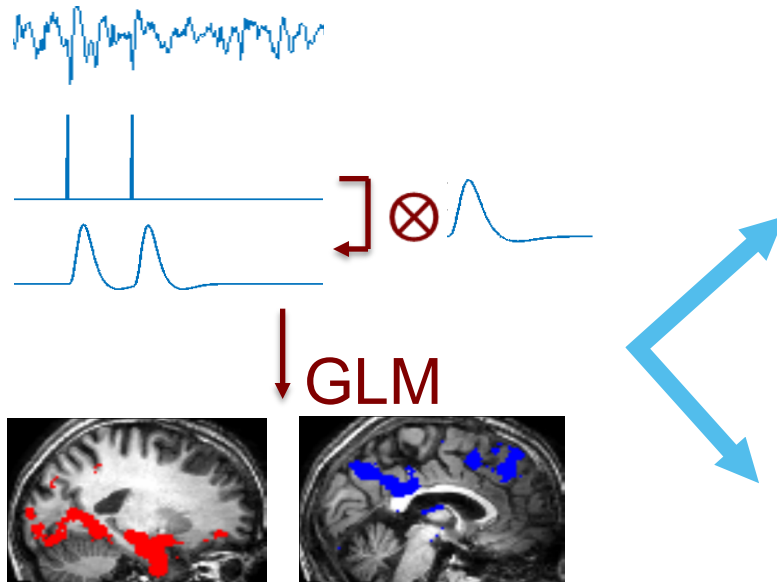
Related to epilepsy:
[Zhang et al. 2009]

Tensor-based fMRI analysis

- Tensor-PICA [Beckmann&Smith2005]:
 - Extension of previous model for multisession fMRI
 - Sessions have equal time courses (task-based fMRI)
 - Voxel x time x sessions OR voxel x time x subjects
 - CPD with independence constraint
- BTD-(L,L,1) for spatially folded fMRI [Chatzichristos2017]

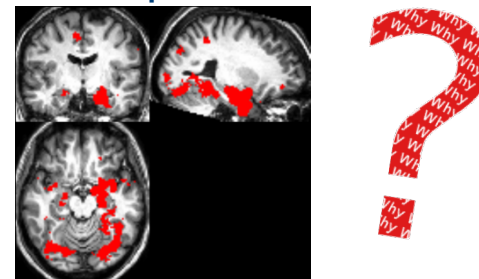


EEG-correlated fMRI



40-70% EEG-fMRI studies fail
due to lack of interictal spikes
[Grouiller et al. Brain 2011]

Widespread activation



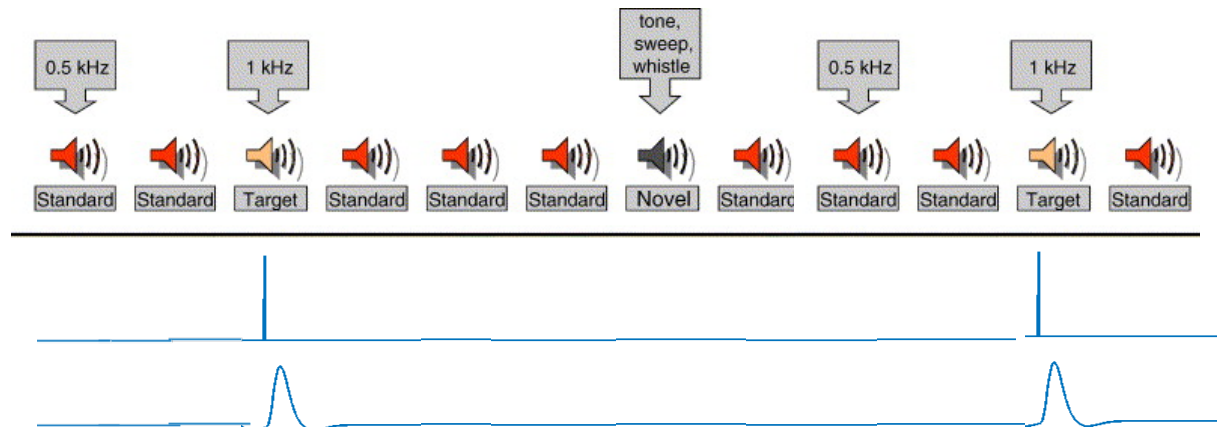
We need better spatiotemporal resolution

- Symmetric EEG-fMRI integration
- Find a common mode of variation
- Joint decomposition (BSS) where signatures in this mode are shared
 - Subject / patient
 - JointICA
 - Multichannel jointICA
 - CPD
 - Time

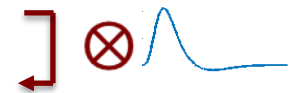
We need better spatiotemporal resolution

- Symmetric EEG-fMRI integration
- Find a common mode of variation
- Joint decomposition (BSS) where signatures in this mode are shared
 - **Subject / patient**
 - JointICA
 - Multichannel jointICA
 - CPD
 - Time

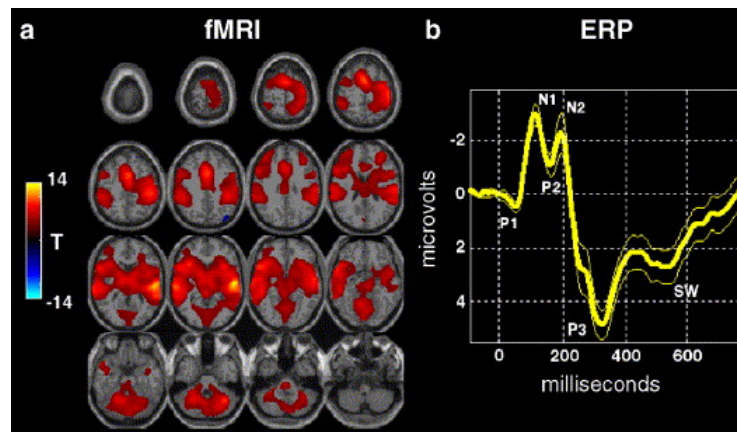
Study cognitive function with EEG-fMRI



Peak at 5s!



GLM



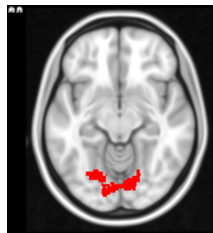
[Calhoun2006]

EEG-fMRI fusion via BSS

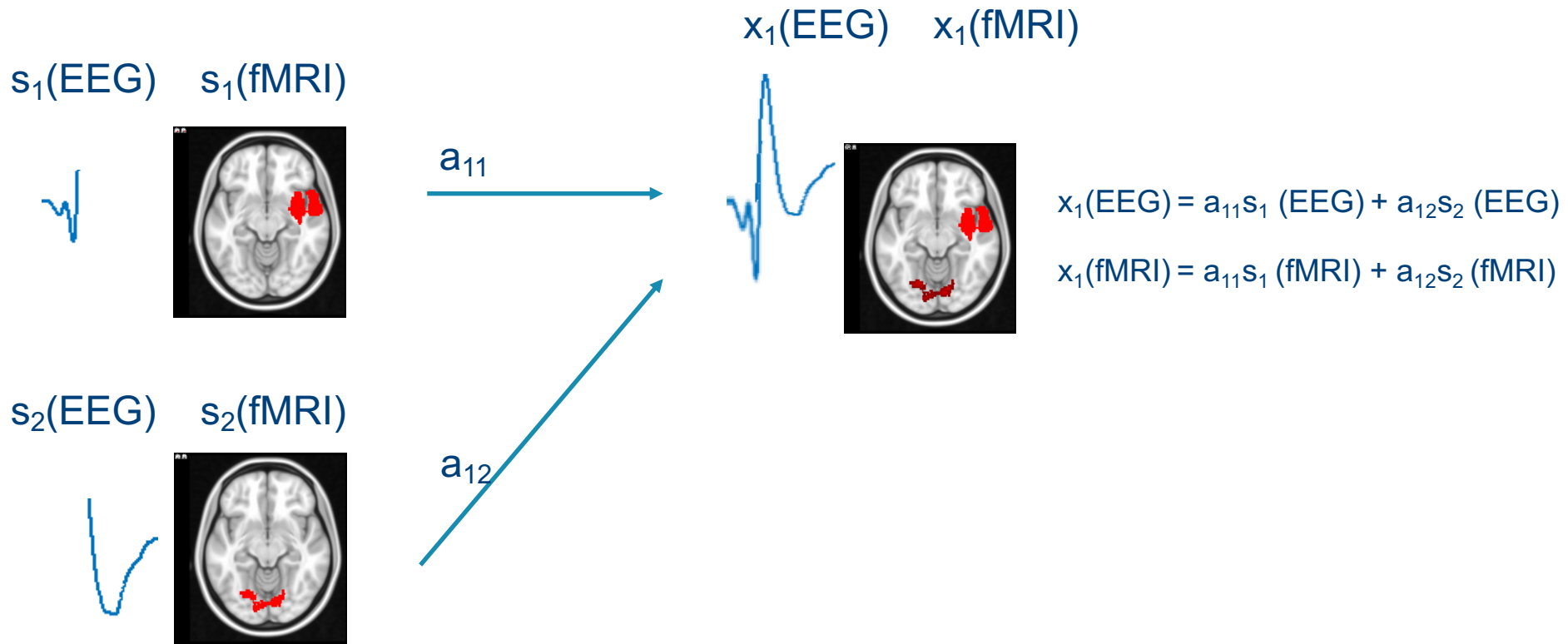
$s_1(\text{EEG})$ $s_1(\text{fMRI})$



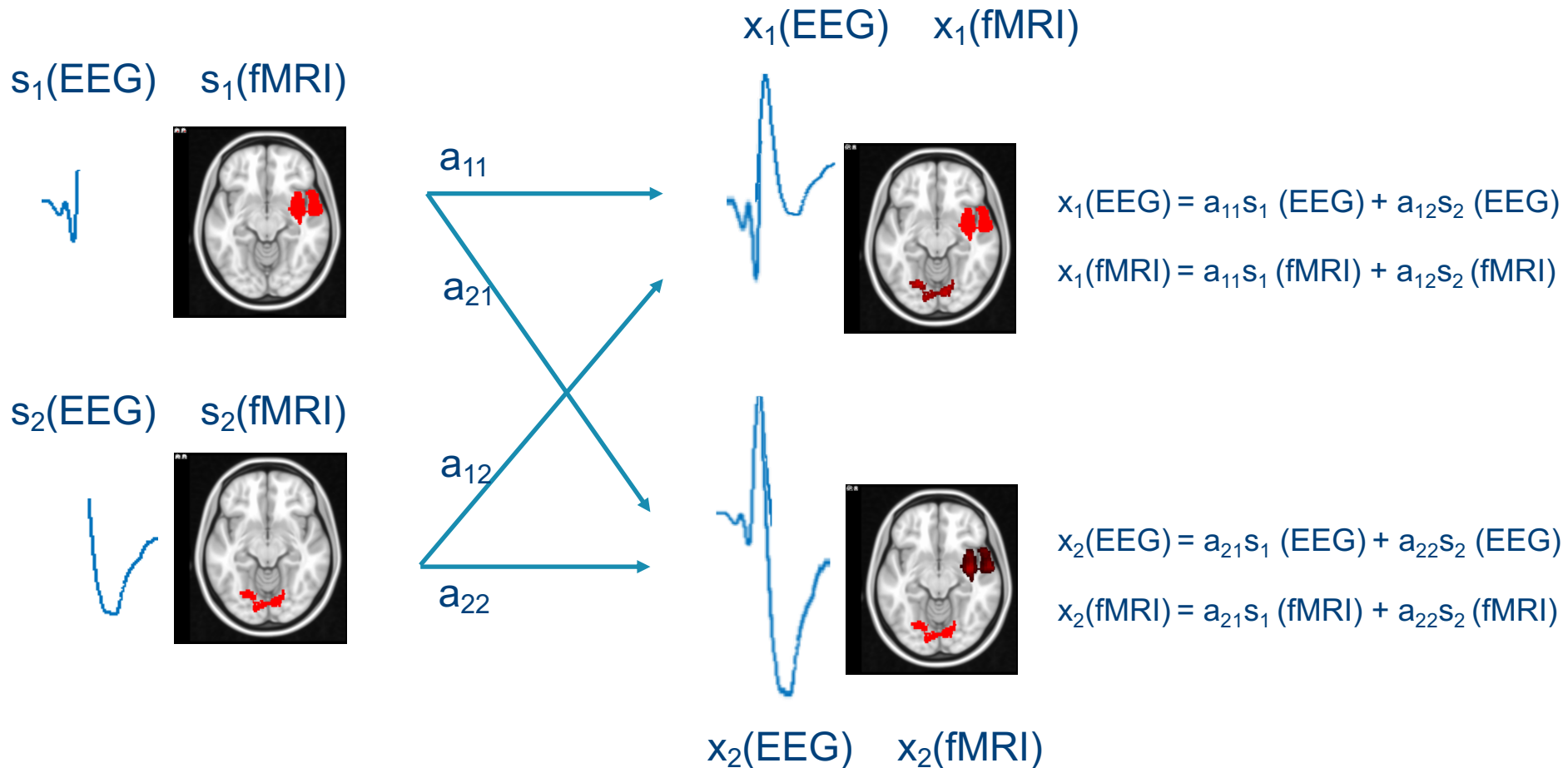
$s_2(\text{EEG})$ $s_2(\text{fMRI})$



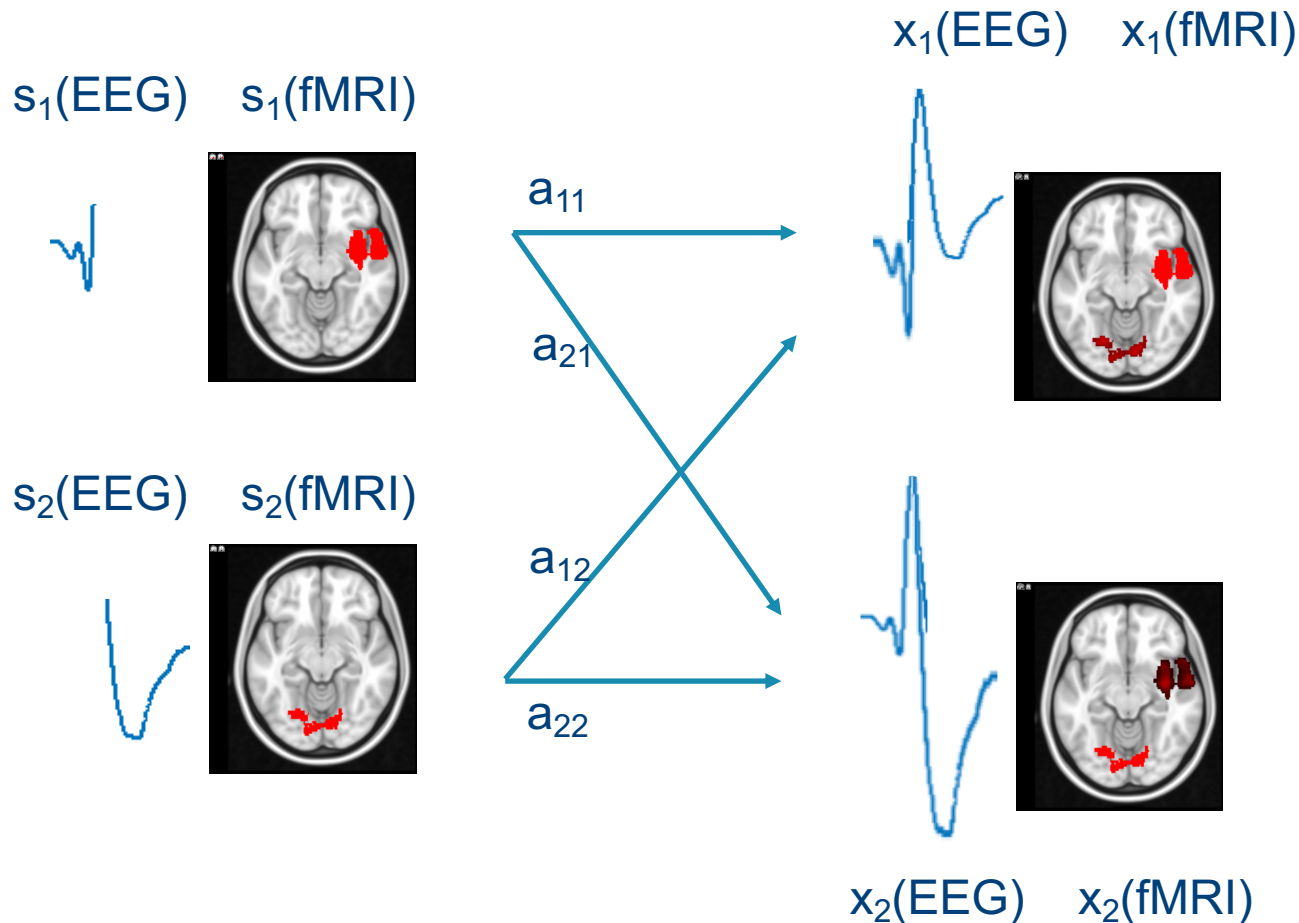
EEG-fMRI fusion via BSS



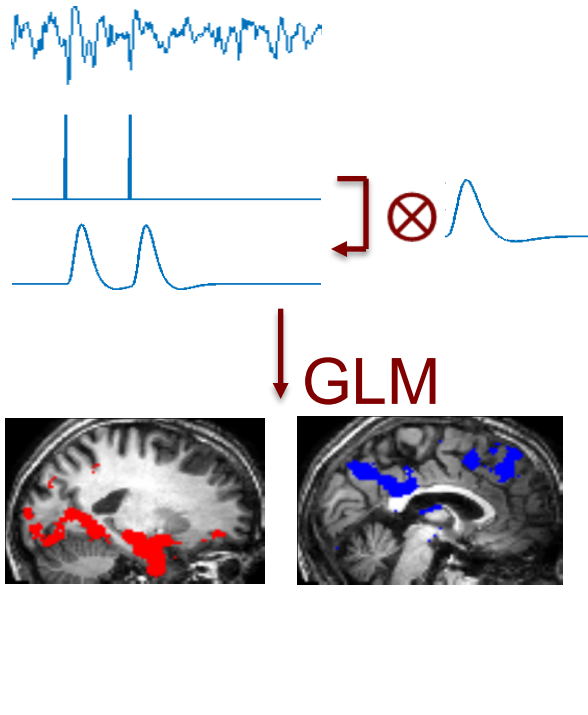
EEG-fMRI fusion via BSS



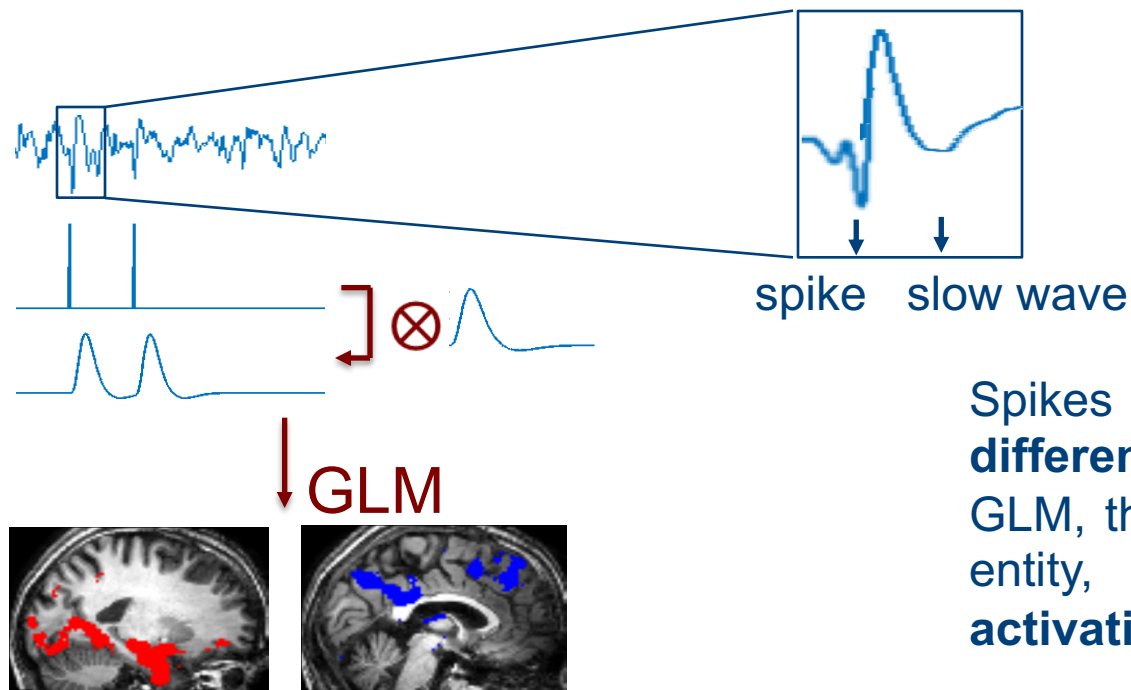
EEG-fMRI fusion via BSS



EEG-correlated fMRI



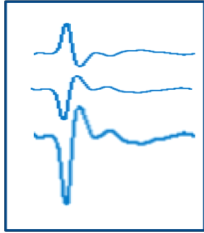
Traditional GLM-based analysis



Spikes and slow waves reflect **different neural processes**. In GLM, they are **modelled as one entity**, causing **widespread activation**.

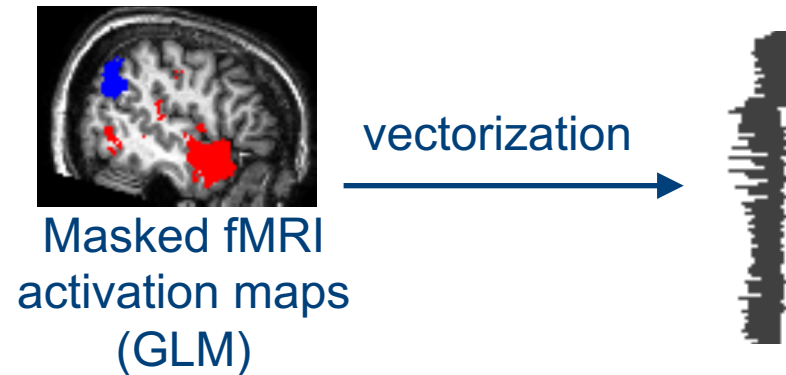
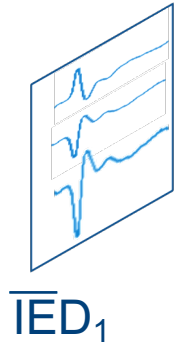
Goal: Disentangle the different neural processes from multisubject **EEG-fMRI** in order to obtain a better spatiotemporal characterization

Data representation

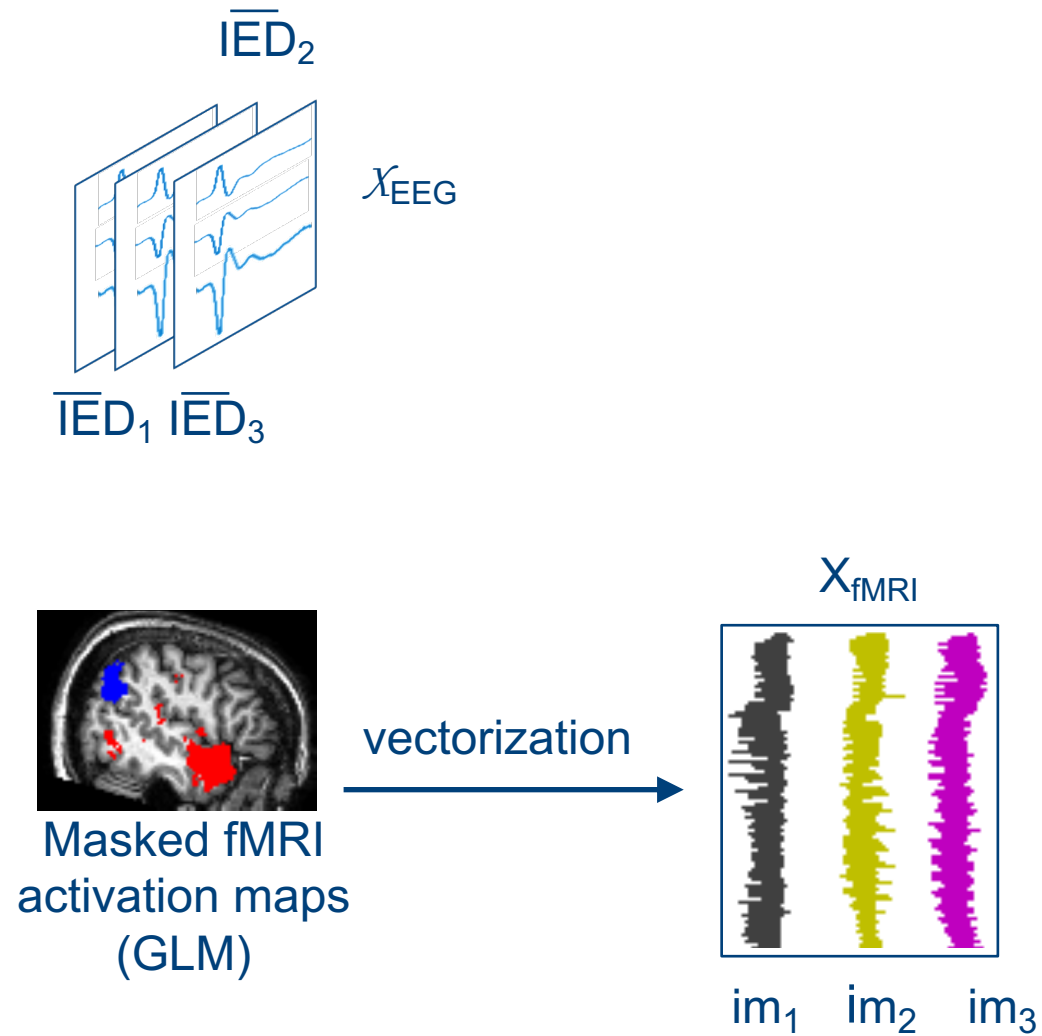


$\overline{\text{IED}}_1$

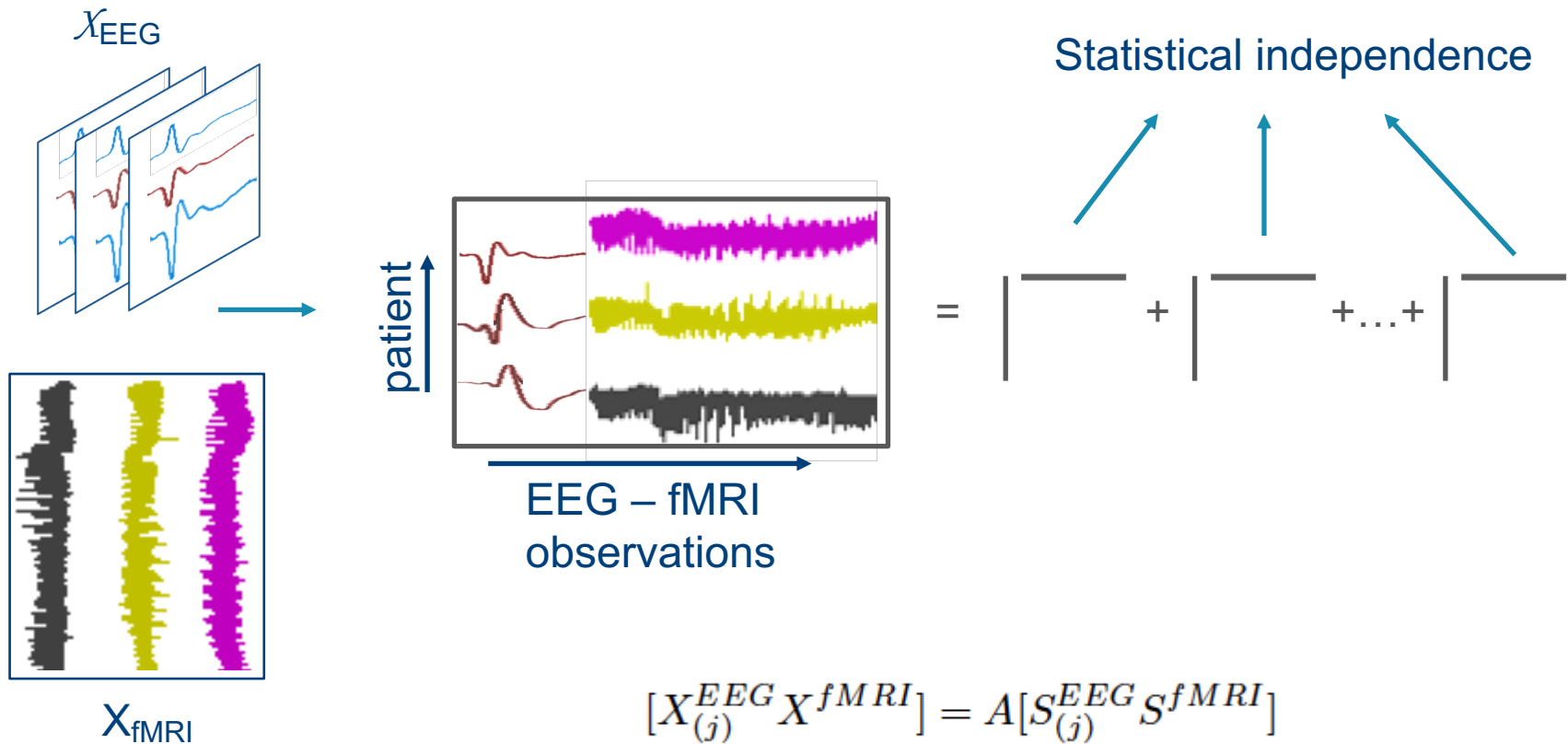
Data representation



Data representation

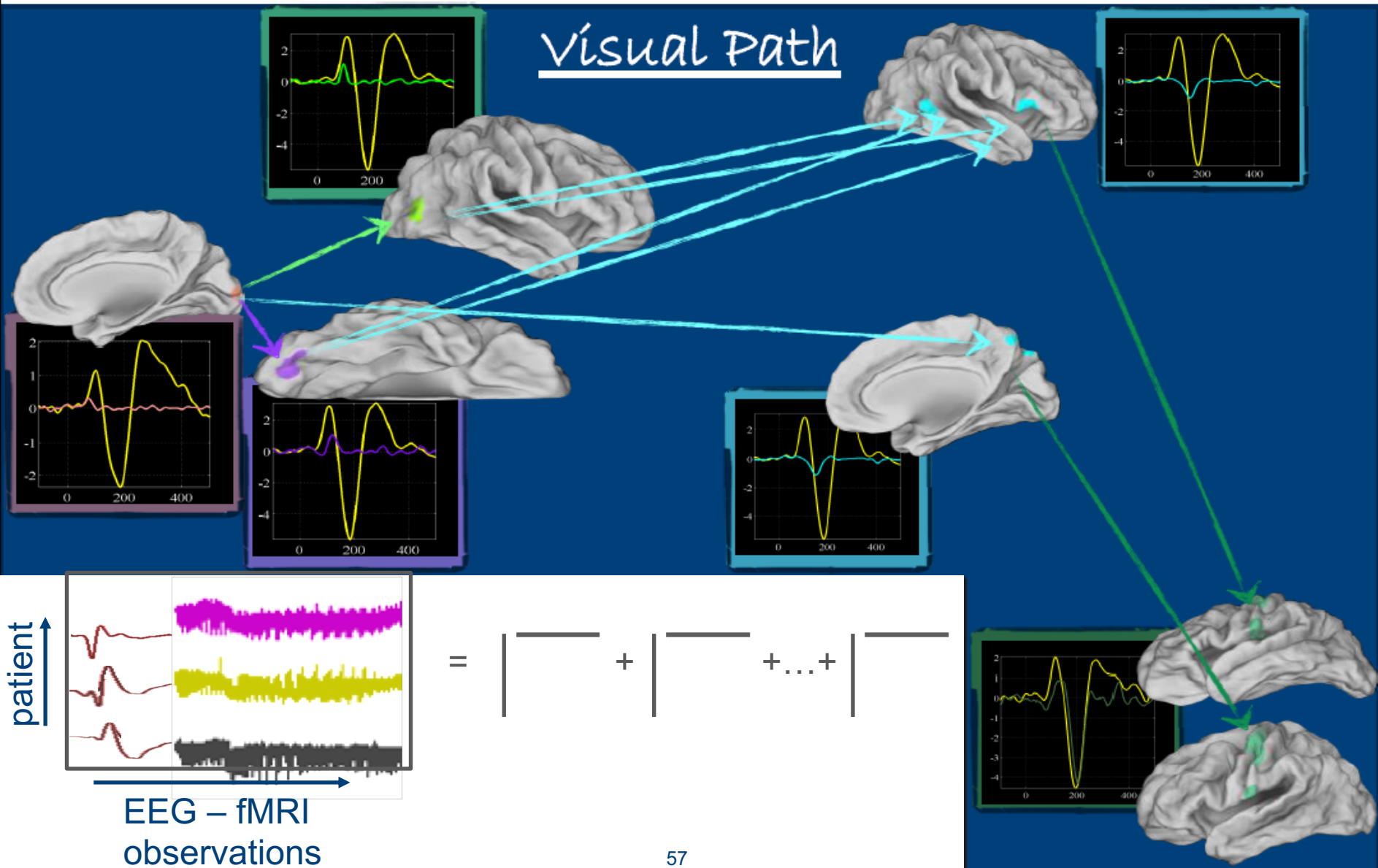


Joint blind source separation (1): jointICA

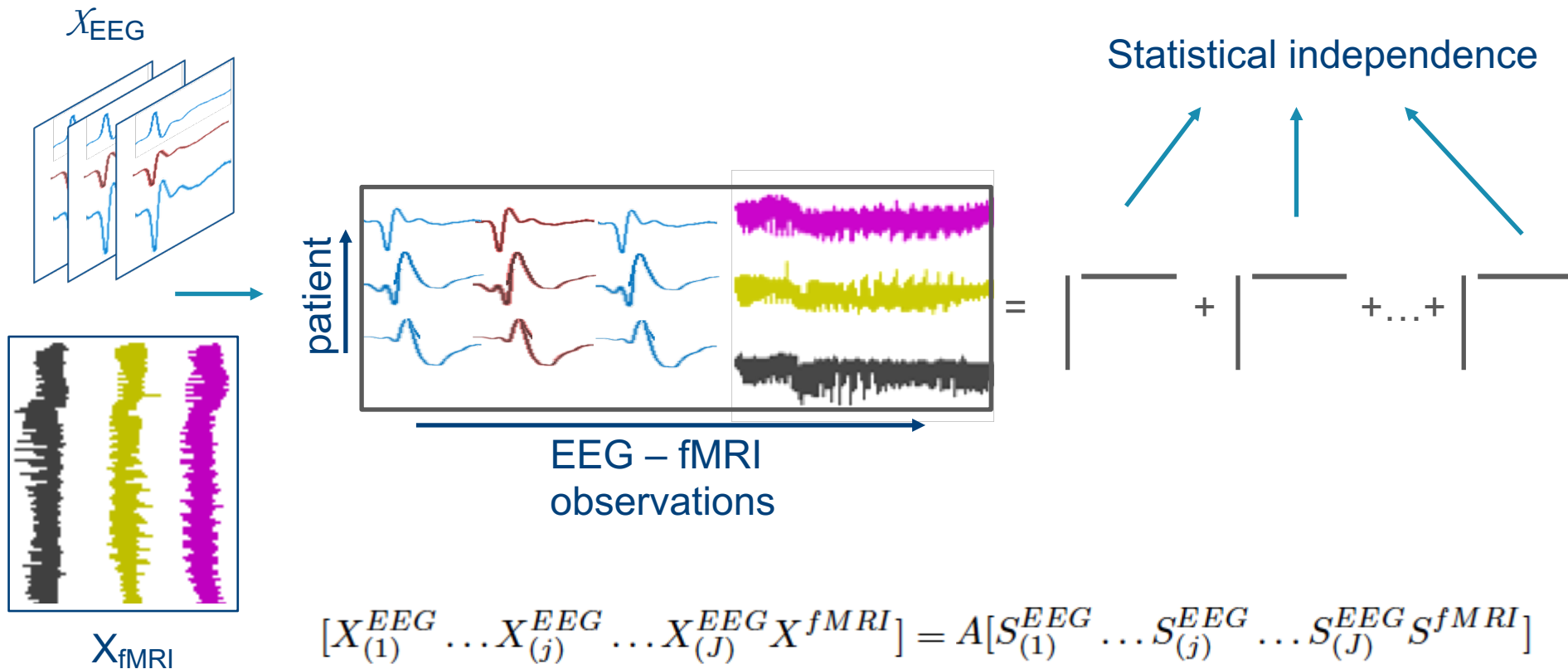


[Calhoun 2006]

JointICA: Visual detection task [Mijovic 2012]



Joint blind source separation (2): t-jointICA



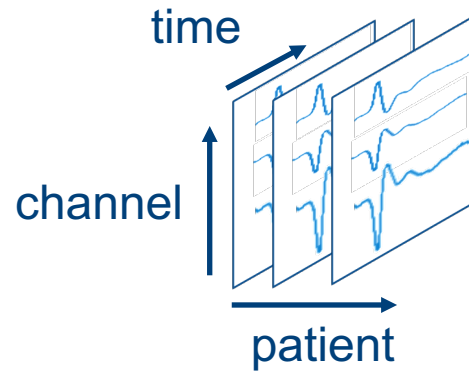
$$[X_{(1)}^{EEG} \dots X_{(j)}^{EEG} \dots X_{(J)}^{EEG} X^{fMRI}] = A[S_{(1)}^{EEG} \dots S_{(j)}^{EEG} \dots S_{(J)}^{EEG} S^{fMRI}]$$

[Swinnen 2014]

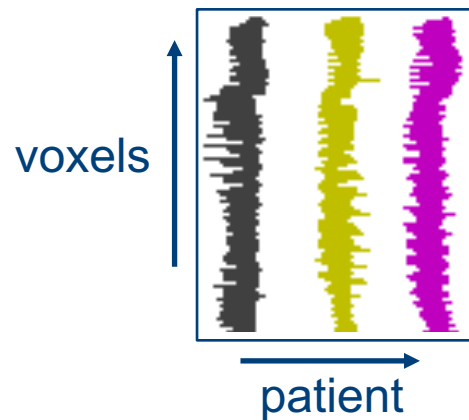
58

KU LEUVEN

Joint blind source separation (3): Coupled tensor-matrix factorization



$$= \begin{array}{|c|} \hline \text{red line} \\ \hline \end{array} + \begin{array}{|c|} \hline \text{green line} \\ \hline \end{array} + \dots + \begin{array}{|c|} \hline \text{purple line} \\ \hline \end{array}$$



$$= \begin{array}{|c|} \hline \text{red line} \\ \hline \end{array} + \begin{array}{|c|} \hline \text{green line} \\ \hline \end{array} + \dots + \begin{array}{|c|} \hline \text{purple line} \\ \hline \end{array}$$

$$f(A, P, Q, S^{fMRI}) = \\ = \|X^{fMRI} - AS^{fMRI}\|^2 + \|\mathcal{X}^{EEG} - \sum_R \mathbf{a}_r \circ \mathbf{p}_r \circ \mathbf{q}_r\|^2$$

[Acar 2014, Hunyadi 2016]

Experiments

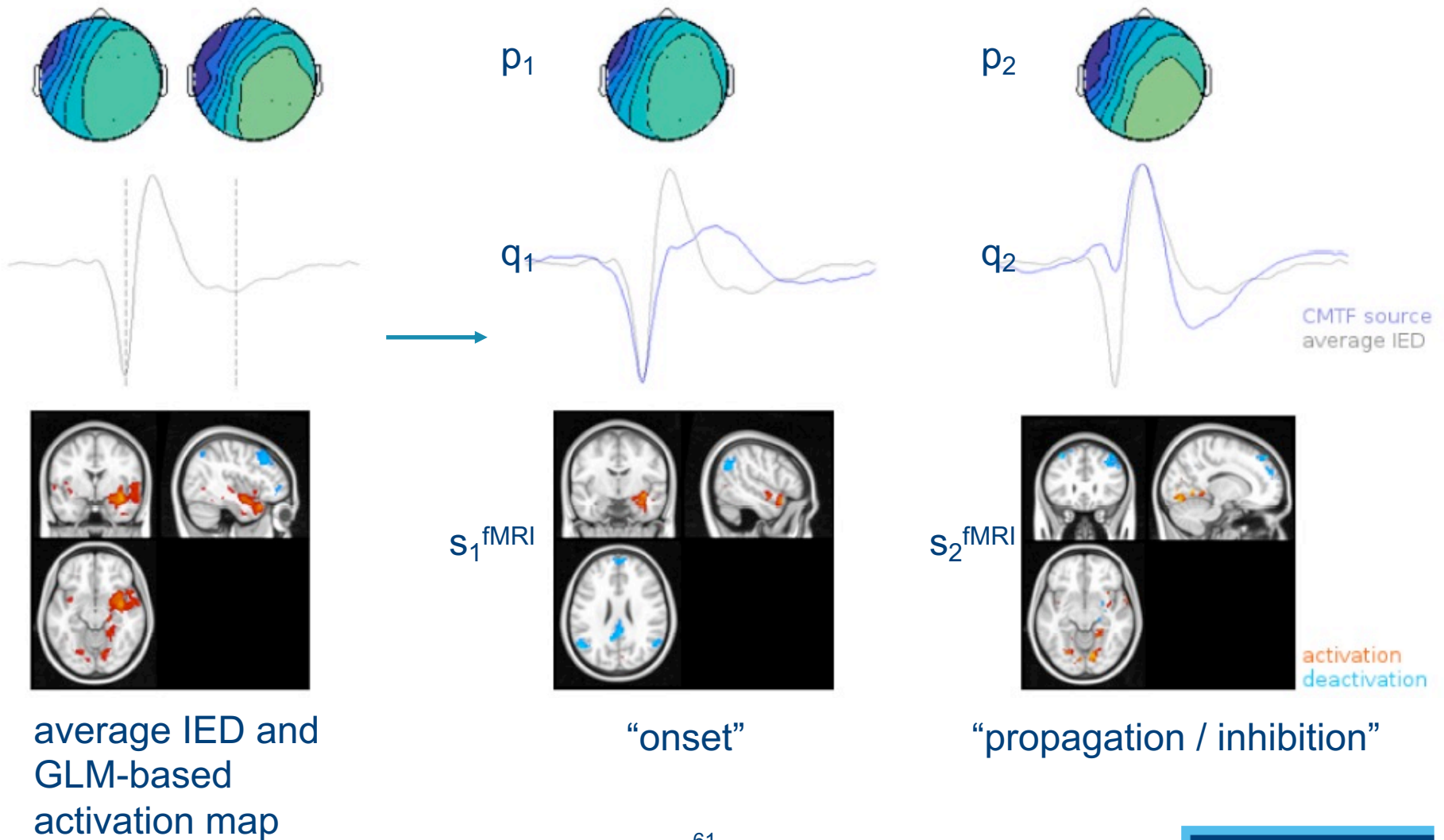
Dataset

- 10 temporal lobe epilepsy (TLE) patients, 5 right, 5 left
- To get a consistent set, the EEG and the fMRI of the LTLE patients are mirrored

Model selection

- $R=2$ was chosen

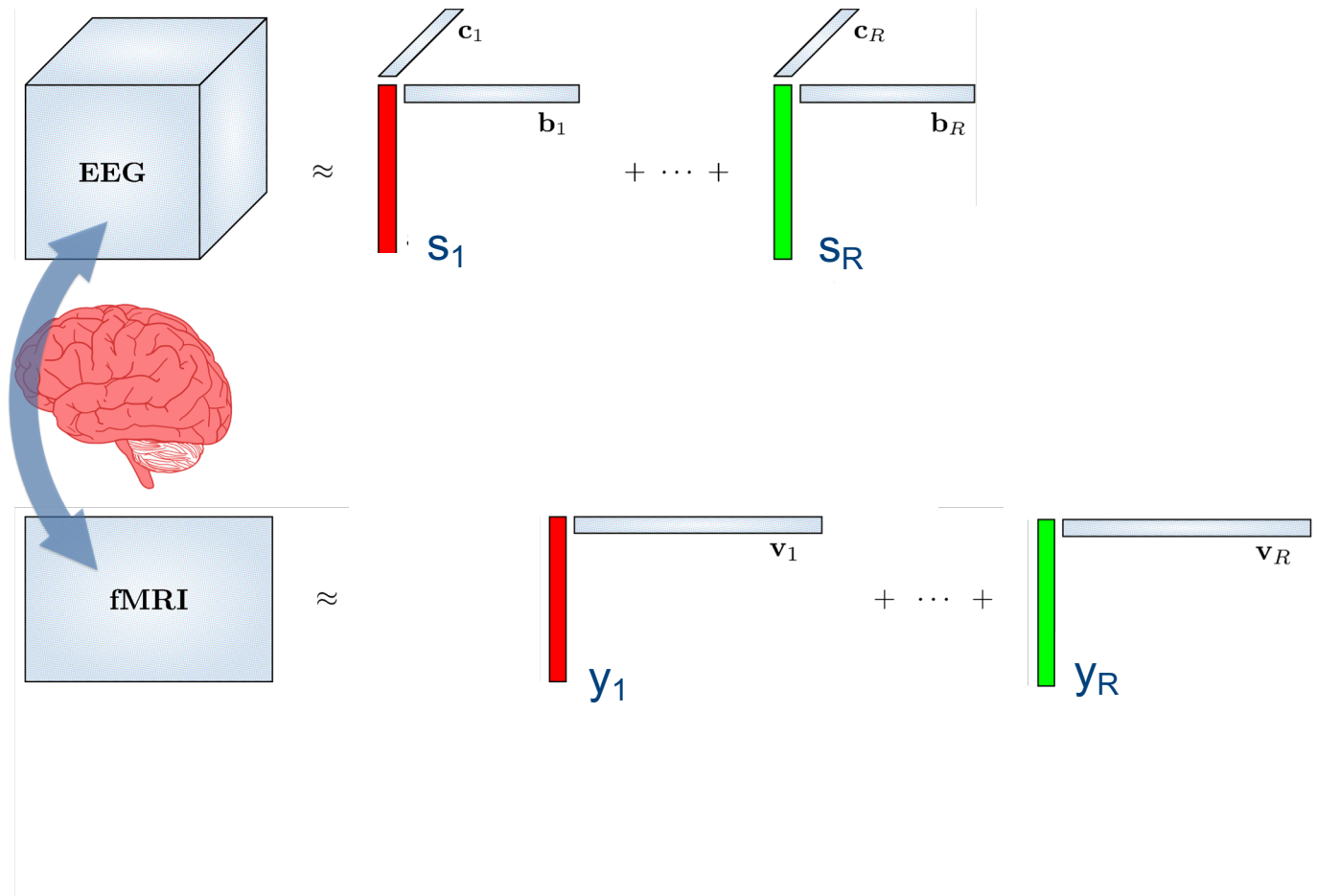
Results: epileptic network



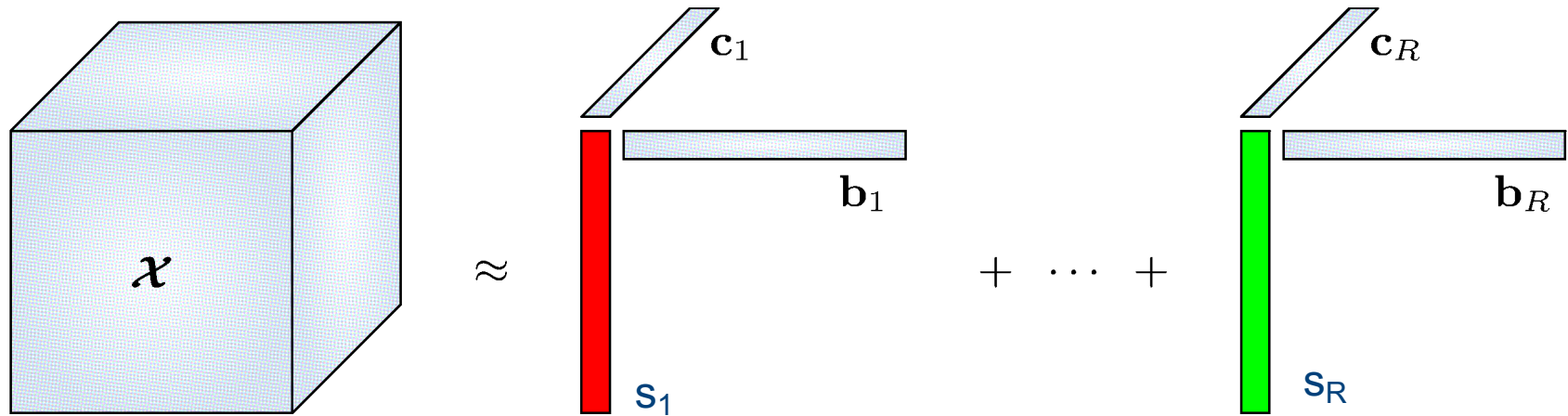
We need better spatiotemporal resolution

- Symmetric EEG-fMRI integration
- Find a common mode of variation
- Joint decomposition (BSS) where signatures in this mode are shared
 - Subject / patient
 - JointICA
 - Multichannel jointICA
 - CPD
 - **Time**

EEG-fMRI fusion in the temporal mode



The proposed approach



EEG decomposed into components

1 component / source = temporal pattern (s)
+ activity over channels (b)
+ activity over frequencies (c)

Hemodynamic coupling

$$y(t) = h(t) * s(t)$$

modelled time course in 1 voxel

$$y(t) = \sum_{u=1}^L h(t-u)s(u)$$

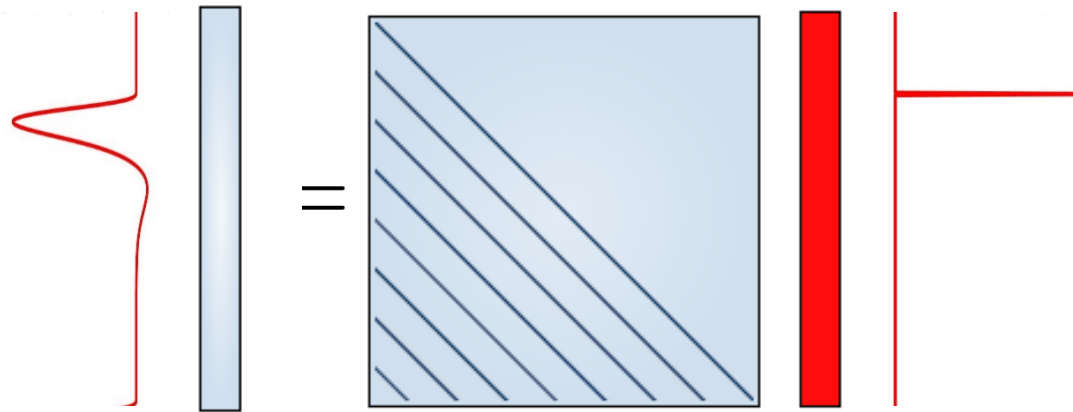
$$\begin{bmatrix} y(0) \\ y(1) \\ y(2) \\ \vdots \\ y(N) \end{bmatrix} = \begin{bmatrix} h(0) & 0 & 0 & \cdots & 0 & 0 \\ h(1) & h(0) & 0 & \cdots & 0 & 0 \\ h(2) & h(1) & h(0) & \cdots & 0 & 0 \\ \vdots & \vdots & \vdots & \ddots & \vdots & \vdots \\ h(N) & h(N-1) & h(N-2) & \cdots & h(1) & h(0) \end{bmatrix} \begin{bmatrix} s(0) \\ s(1) \\ s(2) \\ \vdots \\ s(N) \end{bmatrix}$$

Hemodynamic coupling

$$y(t) = h(t) * s(t)$$

$$y(t) = \sum_{u=1}^L h(t-u)s(u)$$

modelled time course in 1 voxel

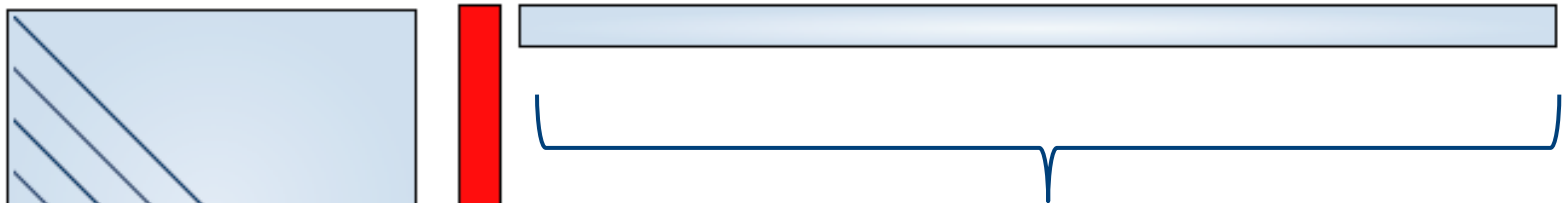


Hemodynamic coupling

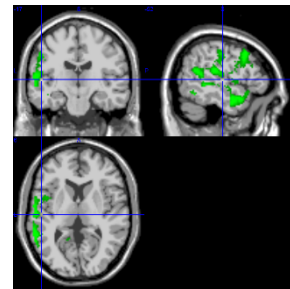
$$y(t) = h(t) * s(t)$$

$$y(t) = \sum_{u=1}^L h(t-u)s(u)$$

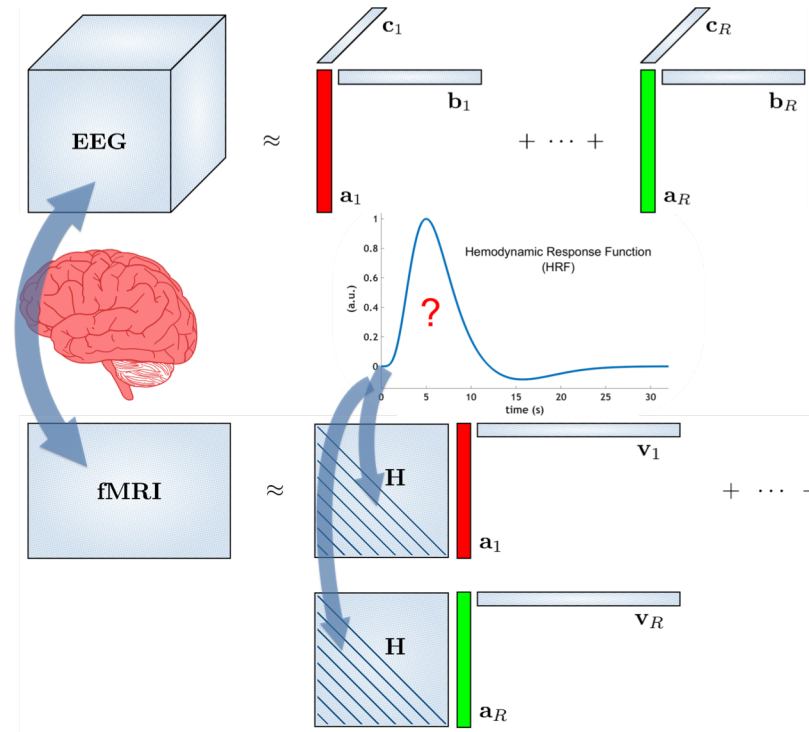
modelled time course in 1 voxel



activation pattern over voxels



EEG-fMRI fusion in the temporal mode



$$J(\mathbf{A}, \mathbf{B}, \mathbf{C}, \mathbf{V}, \theta) = \left\| \mathcal{X} - \sum_{r=1}^R \mathbf{a}_r \otimes \mathbf{b}_r \otimes \mathbf{c}_r \right\|^2 + \quad (3)$$

$$\left\| \mathbf{Y} - \sum_{r=1}^R (\mathbf{H}(\theta) \mathbf{a}_r) \otimes \mathbf{v}_r \right\|^2, \text{ s.t. } \mathbf{A}, \mathbf{C} \geq 0$$

[Van Eyndhoven 2016]

KU LEUVEN

Advantages of the approach

In a simulation study, it was shown that

- Proposed approach can estimate subject-specific HRF
- Accounting for HRF variability results in more accurate characterization of neural sources of activity
 - In spatial / temporal / spectral domain
- Proposed approach can deal with
 - different changes in HRF waveform
 - spatially / temporally correlated noise

Summary

- EEG and fMRI measure a mixture of brain and non-brain sources, resulting in low SNR
- Tensor-based blind source separation is a powerful way to deal with this problem
- Successful applications in EEG and in fMRI
- Fusion of EEG-fMRI for better spatiotemporal resolution
- Tensor-based fusion along a common mode of variation



Thank you!

Acknowledgments

- | University Hospitals Leuven Gasthuisberg
- | KU Leuven, Dept. Electrical Engineering-ESAT, division STADIUS
- | KU Leuven, Dept. of Psychology
- | University of Oxford, Institute of Biomedical Engineering
- | Universidad de Oriente, Cuba



ERC advanced grant 339804 BIOTENSORS in collaboration with L. De Lathauwer and group



27-08-18